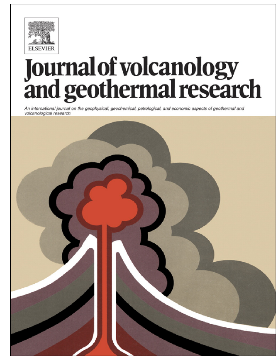


# Results of the CO2 diffuse degassing survey from the 2017 IAVCEI CCVG 13th volcanic gas workshop: Pululahua dome complex, Ecuador

M.C. Lamberti, D. Sierra, C. Cardellini, F. Viveiros, A. Vásconez Müller, F.J. Vasconez, D.F. Narváez, C. Silva, G. Melián, S. Caliro, B.M. Kis, A. Ionescu, S. Hidalgo

PII: S0377-0273(24)00137-9

DOI: https://doi.org/10.1016/j.jvolgeores.2024.108145

Reference: VOLGEO 108145

To appear in: *Journal of Volcanology and Geothermal Research*

Received date: 22 March 2024

Revised date: 11 July 2024

Accepted date: 23 July 2024

Please cite this article as: M.C. Lamberti, D. Sierra, C. Cardellini, et al., Results of the CO2 diffuse degassing survey from the 2017 IAVCEI CCVG 13th volcanic gas workshop: Pululahua dome complex, Ecuador, *Journal of Volcanology and Geothermal Research* (2024), https://doi.org/10.1016/j.jvolgeores.2024.108145

# Results of the $CO_2$ Diffuse Degassing Survey from the 2017 IAVCEI CCVG 13th Volcanic Gas Workshop: Pululahua Dome Complex, Ecuador

Lamberti, M.C.[1,2]*, Sierra, D.[3], Cardellini, C.[4,5], Viveiros, F.[6,7], Vásconez Müller, A.[3,8], Vasconez, F.J.[3,8], Narváez, D.F.[9], Silva, C.[6,10], Melián, G.[11,12], Caliro, S.[13], Kis, B.M.[14,15,16], Ionescu, A.,[4,14,15,17], Hidalgo, S.[3]

[1]Departamento de Ciencias Geológicas, Facultad de Ciencias Exactas y Naturales, Universidad de Buenos Aires, Buenos Aires, Argentina

[2]Instituto de Estudios Andinos "Don Pablo Groeber" (IDEAN), CONICET—Universidad de Buenos Aires, Buenos Aires, Argentina

[3]Instituto Geofísico de la Escuela Politécnica Nacional, Quito, Ecuador

[4]Università degli Studi di Perugia, Dipartimento di Fisica e Geologia, Perugia, Italy

[5]Istituto Nazionale di Geofisica e Vulcanologia, Sezione di Bologna, Bologna, Italy

[6]IVAR - Research Institute for Volcanology and Risks Assessment, University of the Azores, Ponta Delgada, Portugal

[7]FCT - Faculty of Sciences and Technology, University of the Azores, Ponta Delgada, Portugal

[8]School of Earth Sciences, University of Bristol, Bristol, BS8 IRJ, UK

[9]Departamento de Geología, Facultad de Ingeniería en Geología y Petróleos, Escuela Politécnica Nacional, Quito, Ecuador

[10]CIVISA - Centro de Informação e Vigilância Sismovulcânica dos Açores, Ponta Delgada, Portugal

[11]Instituto Volcanológico de Canarias (INVOLCAN), Santa Cruz de Tenerife, Spain

[12]Instituto Tecnológico y de Energías Renovables (ITER), Santa Cruz de Tenerife, Spain

[13]Istituto Nazionale di Geofisica e Vulcanologia, "Osservatorio Vesuviano", Napoli, Italy

[14]Babeș-Bolyai University, Faculty of Biology and Geology, Cluj-Napoca, Romania

[15]HUN-REN, Institute for Nuclear Research, Debrecen, Hungary

[16]HUN-REN-ELTE Volcanology Research Group, Eötvös University, Budapest, Hungary

[17]Babeș-Bolyai University, Faculty of Environmental Science and Engineering, Cluj-Napoca, Romania

*Corresponding author.*

• E-mail address: mclamberti@gl.fcen.uba.ar

• Full postal address: 5598 Francisco Borges, Buenos Aires, 1605, Argentina.

**Abstract**

Pululahua is a potentially active andesite and dacite lava dome complex. This paper presents the results of a survey focused on carbon dioxide ($CO_2$) diffuse degassing at Pululahua, which was conducted during the 2017 International Association of Volcanology and Chemistry of the Earth's Interior (IAVCEI) Commission of the Chemistry of Volcanic Gases (CCVG) 13$^{th}$ Gas Workshop. Our objective was to conduct a comprehensive investigation of $CO_2$ diffuse degassing by employing standard methods for measuring $CO_2$ flux and temperature, and data processing. These methods were applied to map the spatial distribution of the measured parameters, investigate the origin of $CO_2$, and quantify the volcanic $CO_2$ output within the surveyed area of Pululahua. We carried out a total of 350 soil $CO_2$ flux and 329 soil temperature measurements and collected 12 gas samples for carbon isotopic composition analysis, surrounding the three youngest domes in the complex. In addition, seventeen $CO_2$ flux measurements over a thermal water pool were performed. Our findings indicate that the diffuse emission at Pululahua's crater floor is fed by both biogenic and volcanic $CO_2$. Fluxes from each source are similar in magnitude, with approximately 90% of the measurements falling into an intermediate flux range. The occurrence of volcanic $CO_2$ emissions is supported by the carbon isotopic composition. Diffuse degassing distribution highlights a $CO_2$ anomaly surrounding the younger domes within the crater. We estimated the $CO_2$ diffuse emission using both statistical and geostatistical approaches over area of 3.36 km$^2$, resulting in values of 154.2 t d$^{-1}$ and 126.2 t d$^{-1}$ respectively. Based on the geostatistical quantification of the total $CO_2$ emission from soil degassing, Pululahua's crater volcanic $CO_2$ contribution is estimated between 59 and 97 t d$^{-1}$. Finally, the potential hazards associated with the release of cold $CO_2$ at Pululahua's crater are also discussed.

*Keywords: Pululahua volcano; $CO_2$ diffuse degassing; $CO_2$ sources; soil temperature; diffuse degassing map; CCVG Workshop.*

## 1 Introduction

Every three years, the International Association of Volcanology and Chemistry of the Earth's Interior (IAVCEI) Commission on the Chemistry of Volcanic Gases (CCVG) organizes a Volcanic Gas Workshop. These meetings allow the international scientific community to discuss state-of-the-art knowledge on magmatic volatiles, share case studies of volcanic emissions during eruptive, unrest, and quiescence periods, and share the most modern advances on measurement instruments and techniques. These workshops constitute a unique opportunity for scientists worldwide to gather in the field and carry out observations, deploy remote sensing measurements of volcanic plumes, sample fumaroles and waters, and measure soil diffuse degassing, with the aim of comparing methodologies and techniques and finally integrate their results.

The results of a comparative study of $CO_2$ diffuse degassing at Masaya volcano, carried out at the 8th Volcanic Gas Workshop in Nicaragua and Costa Rica in 2003, was published by Lewicki et al. (2005). This study involved five groups measuring $CO_2$ fluxes using the accumulation chamber method (Chiodini et al. 1998) at the same locations both in the morning and afternoon, to compare measurements under diverse daytime and meteorological conditions. They also compared different geostatistical methods to map $CO_2$ flux and estimate the total $CO_2$ emission, using a single data set. Among these, the sequential Gaussian simulation method (e.g., Cardellini et al., 2003) was found to yield the most realistic representation of the spatial distribution of $CO_2$ diffuse degassing. They noted the high sensitivity of $CO_2$ fluxes to temporal fluctuations, largely attributed to meteorological effects on gas flow through permeable pathways.

More recently, Lopez et al. (2018) presented the main results of integrated sampling during the 12th Volcanic Gas Workshop held in Chile in 2014, at Lastarria volcano. On that occasion, the main goal was to estimate the total $CO_2$ emitted to the atmosphere using different sampling techniques, as well as to refine the existing subsurface models for Lastarria volcano, and provide new constraints on its magmatic-hydrothermal system and total degassing budget.

During the 13th CCVG Gas Workshop held in Ecuador in 2017 (https://ccvg.iavceivolcano.org/field-workshops/workshop-2010-2017), the $CO_2$ diffuse degassing CCVG working group carried out a joint campaign at Pululahua volcano (Fig. 1).

Considering that, since the 8th CCVG Volcanic Gas Workshop, methods to investigate $CO_2$ diffuse degassing have become more tested and widely used worldwide, the 13th CCVG Volcanic Gas Workshop provided an excellent opportunity for multiple research groups to leverage their instruments to conduct a detailed study of a volcanic area of interest, such as Pululahua.

In the Pululahua survey, we used five different portable soil $CO_2$ fluxmeter devices, belonging to IG-EPN (Ecuador), University of Perugia (Italy), IVAR-University of the Azores (Portugal), Instituto Tecnológico y de Energías Renovables/Instituto Volcanológico de Canarias (ITER/INVOLCAN, Spain), and Babeș-Bolyai University (Cluj-Napoca, Romania) (Fig. 1-A).

Pululahua is a potentially active lava dome complex (Hall, 1977), whose first hazard map was published by Hall and von Hillebrandt in 1988. Pululahua is composed of over a dozen lava domes and a 13 $km^2$ crater (Fig. 1-C&D). Its eruptive history during the Holocene was characterised by effusive dome building and explosive dome destruction eruptions, some of which of Plinian-type magnitude and being its last eruptive period in 2200 BP (Papale and Rosi, 1993; Pallini, 1996; Andrade, 2002; Volentik et al., 2010, Vásconez Müller et al., 2022). Over the last three decades Pululahua's activity consisted of low levels of seismicity, a hydrothermal spring and some $CO_2$ degassing areas (IG-EPN-2016; Andrade et al., 2021), which all indicate that the dome complex is currently in a state of quiescence. Nevertheless, considering the proximity (~15 km) of Pululahua volcano to Quito, the capital city, the presence of critical infrastructure, the permanent population living inside the crater, and the large number of tourists yearly visiting this area, studies to evaluate its present volcanic activity are necessary.

The first $CO_2$ diffuse degassing survey at Pululahua was performed by Padrón et al. (2008). The authors performed 217 measurements, by using the accumulation chamber method, covering an area of about 27.6 $km^2$. The highest $CO_2$ fluxes were measured around the Pondoña and Rumiloma domes, the youngest domes of the volcanic complex (Fig. 1-C and D) and a $CO_2$ emission rate of 270 t $d^{-1}$ was estimated (Padron et al., 2008).

In this work, we present the results of the collaborative field work and data analysis, performed in the framework of the 13th CCVG Gas Workshop, consisting of i) detailed maps of the soil $CO_2$ diffuse degassing and soil temperature of the area around the youngest Pondoña and Rumiloma domes, ii) the quantification of the $CO_2$ total diffuse emission from the study area and iii) a novel investigation of the origin of the $CO_2$ at Pululahua, based on the carbon isotopic composition of released $CO_2$. Finally, this study evaluates the potential hazards posed by $CO_2$ at the inhabited Pululahua crater. This work provides valuable information about $CO_2$ degassing at Pululahua Dome Complex, establishing a baseline for future monitoring efforts.

## 2 Environmental setting

### 2.1 Geological setting

The Ecuadorian volcanic arc is characterised by the presence of more than 80 Plio-Quaternary volcanoes, 21 of which show a degree of activity (Fig. 1-B, Hall et al., 2008; Bernard and Andrade, 2011; Santamaría et al., 2017; Ramon et al., 2021; Hidalgo et al., 2024). Volcanism in this segment occurs due to the subduction of the oceanic Nazca plate beneath the South American continental plate (Barberi et al., 1988; Gutscher et al., 1999; Bourdon et al., 2003). Pululahua is located on the Volcanic Front along with other active volcanoes, such as Chiles-Cerro Negro, Cuicocha, Guagua Pichincha, and Quilotoa (Hall et al., 2008, Bernard and Andrade, 2011; Ramon et al., 2021).

Regarding the tectonic setting, Pululahua is located in the Ecuadorian geologic province of the Western Cordillera (Hall and Beate, 1991; Eguez and Albán, 2017). The area in which this dome complex was emplaced is controlled by two main regional faults: the Quito fault system and the Nono fault (Alvarado et al., 2014; Fig. 1-C). The first one is an active, 40-km-long, reverse structure that terminates just east of Pululahua, while the second one is a dextral transpressive system. The Nono fault belongs to the Quito-Latacunga fault zone, a set of compressive structures located at the east of the major dextral system that governs the movement of almost the entire portion of the northern Andes (Ego et al., 1996; Eguez et al., 2003; Alvarado et al., 2014; Yepez et al., 2016).

Pululahua is an extensive volcanic complex composed of sixteen dacitic-andesitic lava domes located inside and around a semi-rectangular depression (Fig. 1-C&D). Its geologic history is divided into three main stages: (1) a first period characterised by effusive lava dome growth (Units I and II, >18 - 12 ka; Andrade et al., 2021), (2) a second period that initiated with a Plinian-type eruption (VEI 4, Papale and Rosi 1993) and continued with at least four phases of ephemeral dome growth and their subsequent explosive destruction, responsible for the formation of the sub-rectangular 3-km-wide depression (Unit III, 2.6 – 2.3 ka BP; Vásconez Müller et al., 2022), and (3) a final period encompassing partially explosive dome growth inside the depression (Unit IV, 2.2 ka BP; Andrade et al., 2021).

The first stage, also referred to as the pre-Holocene period, is characterised by effusive eruptions of dacitic lavas. Its volcanic products are depicted in the map of Fig. 1-C as pre-crater domes and associated pyroclastic deposits (Andrade et al., 2021). The second stage is defined by the formation of the Pululahua crater, which is associated with several explosive eruptions and ignimbrites (Andrade et al., 2021; Vásconez Müller et al., 2022). The onset of this stage is characterised by discrete phreatomagmatic pulses, which are closely followed by the most voluminous magmatic Plinian-type eruption (Papale and Rosi, 1993; Andrade et al., 2021). The remaining deposits of this member encompass a sequence of Vulcanian ephemeral dome growth and Sub-Plinian to Plinian-type dome destruction events (Vásconez Müller et al., 2022). These members are divided into four distinct eruptive phases by three quiescence periods that were long enough to form incipient soils, which then were buried by hot pyroclastic currents that transformed them into charcoal-rich layers. These volcanic products are depicted in the map of Fig. 1-C as syn-crater ignimbrites. Finally, the third stage is characterised by the extrusion of acidic-andesite lava domes within the crater accompanied by minor explosive events, which formed a crater at the top of Rumiloma domes (Fig. 1-C&D). The cyclic construction/destruction of these three domes (Rumiloma I, Rumiloma II, and Pondoña) led to the formation of thick block-and-ash deposits (>70 meters) that fill the crater floor

(Fig. 1-C; Andrade et al., 2021). These volcanic products are identified in the map of Fig. 1-C and the photo of Fig. 1-D as post-crater domes and associated pyroclastic deposits.

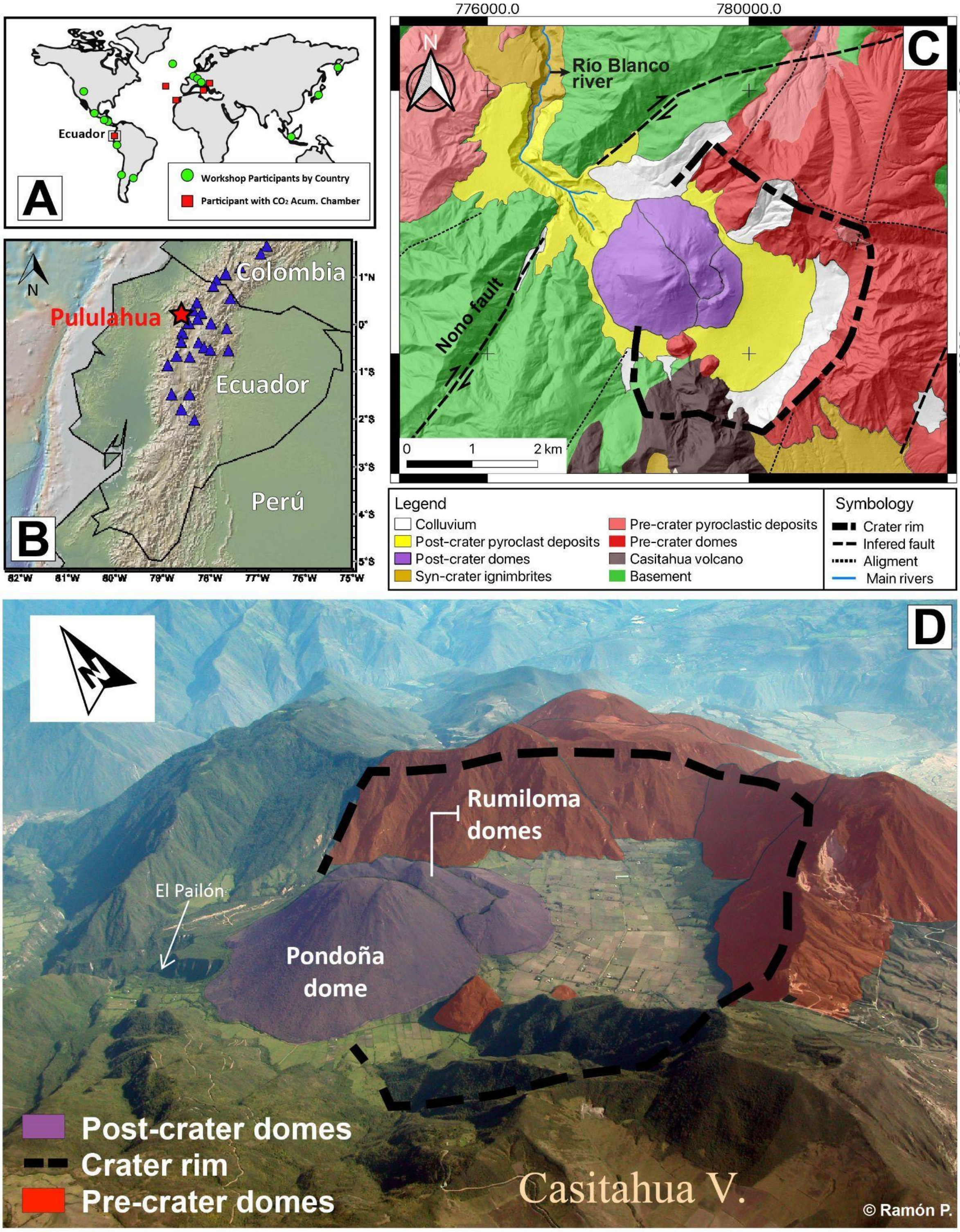


***Figure 1. A***.- *World map showing the location of Ecuador, the workshop hosting country. The locations of the workshop participants (green circles) and of the teams participating in the $CO_2$ diffuse degassing survey (red squares) are also shown.* ***B***.- *Local map of Ecuador with the geographic location of Pululahua volcano in South America (red star). The location of the Quaternary volcanoes*

*of the northern part of South America is also reported (blue triangles). **C**.- Simplified geologic map of Pululahua Dome Complex with its main structures and alignments, modified from Andrade et al. (2021). Map coordinates are expressed in meters, in WGS84 – UTM 17N. **D**.- Pululahua seen from the southwest with its main units and structures. Photo: Ramón, P. (reproduced with permission of the author).*

### 2.2 Hydrothermal activity

Although there are no fumaroles inside the crater, some manifestations of the presence of a hydrothermal system have been reported (IG-EPN, 2016; Andrade et al., 2021). To the west and south of Pondoña dome, there are small depressions characterised by very high emissions of $CO_2$. In fact, in those areas, small animals such as opossums and birds have been found dead, probably associated with asphyxiation due to the high air $CO_2$ concentrations (IG-EPN, 2016). Additionally, the presence of a spring, named “El Pailón”, has been reported in the northwestern area of the crater, at the right margin of Río Blanco river (Fig. 1-D). The “El Pailón” spring water temperature is 25.7°C, which is ~6-7°C higher than that of the adjacent Río Blanco river (Andrade et al., 2021), has a pH of 6.21, a conductivity of 2063 µS/cm (IG-EPN, 2016), and is characterised by the bubbling of gases, reaching $CO_2$ fluxes of about 389 g $m^{-2}$ $d^{-1}$ (Inguaggiato et al., 2010; IG-EPN, 2016).

### 2.3 Microclimates and flora

The study area lies in the Pululahua Geobotanical Reserve. The flora and fauna of this area are particularly diverse (Cerón, 2004, MAATE, 2015). The Reserve is covered by eight microclimates, where the flora is generally composed of trees and shrub vegetation. The area where the diffuse degassing survey was conducted covers the following three microclimates: 1) the Humid Montane Forest located to the west, on Pondoña dome, boasts extraordinary flora diversity due to the high humidity brought in by the western coastal winds; 2) the Semi-dry Montane Forest located to the south of Pondoña and south and east of Rumiloma domes, between the flat part of the base of the domes and their summits, which results from the cold and dry winds coming from the Inter-Andean valley; and, finally, 3) the agricultural lands, where most of the measurement points of this study were conducted, and which have developed at the bottom of the crater and include livestock grazing and agricultural tillage, mainly for traditional crops such as corn and beans, among others (Fig. 1-D).

## 3 Methods

### 3.1 $CO_2$ flux and temperature measurements

$CO_2$ fluxes ($\varphi CO_2$) were measured on the 1st and 2nd of October 2017 with the accumulation chamber method (Chiodini et al., 1998), using five different portable fluxmeters. The fluxmeters were equipped with LICOR LI-800 or LI-820 infrared gas analysers operating in the range of 0 - 20,000 and 0 – 2,000 ppm of $CO_2$. Details on the different devices are reported in Supplementary Material 1.

The repeatability of the $\varphi CO_2$ measurements by the accumulation chamber method was estimated to be around 10% for $CO_2$ fluxes between 10 and 10,000 g $m^{-2}d^{-1}$ by Chiodini et al. (1998). Other studies report measurement uncertainties up to 25% based on measurements at low fluxes (Carapezza and Granieri, 2004). Furthermore, Evans et al. (2001) reported a systematic underestimation of flux (average of -12.5%) over an imposed flux range of 200 to 12,000 g $m^{-2}d^{-1}$. The instruments used in the current study were previously calibrated in each institution laboratory.

Soil temperature was measured at ~10 cm depth using thermometers equipped with metallic probes. Soil gas fluxes and temperatures were measured around Pondoña and Rumiloma domes at 350 and 329 locations, respectively, distributed according to a sampling pattern with a maximum spacing of ~100 m and covering an area of 3.36 $km^2$ (Fig. 2-A). The number of temperature measurements is lower than that of $\varphi CO_2$ measurements due to technical problems with one of the thermometers. Due to the very dense vegetation, which hinders access, the dome area was not surveyed.

Additionally, 17 $CO_2$ flux measurements were taken uniformly on the surface of the water at the “El Pailón” thermal and bubbling pool. For this purpose, the accumulation chamber was replaced by an inverted funnel (volume of 0.0016 $m^3$ and footprint area of 0.03 $m^2$) connected to the flux meter of Babes-Bolyai University (Kis et al., 2017). The total $CO_2$ emission of “El Pailón” was calculated by summing the fluxes measured at each point.

Considering the relevant impact that weather conditions may have on the soil $CO_2$ flux emissions (*e.g.*, Viveiros et al., 2008; Oliveira et al., 2018), all measurements were done in periods under stable weather conditions.

### 3.2 $CO_2$ flux and temperature data analysis

In this study, $CO_2$ flux and temperature data were analysed using two well-established methodologies in the field of spatial data analysis. The Graphical Statistical Approach (GSA; Sinclair, 1974; Chiodini et al., 1998) was used to characterise the statistical distribution of data to investigate the presence of multiple sources of the emitted $CO_2$ and to quantify the $CO_2$ output. The sequential Gaussian simulation (sGs, Deutsch and Journel, 1998; Cardellini et al., 2003, Lewicki et al., 2005) was used to map the spatial distribution of both $CO_2$ flux and soil temperature, and to quantify the $CO_2$ output. Although these methodologies have been extensively discussed in the literature (e.g., Sinclair, 1974; Chiodini et al., 1998; Deutsch and Journel, 1998; Cardellini et al., 2003; Viveiros et al., 2010; Bini et al., 2019, and references therein), it is worth revisiting them to better understand their application in this specific field of study.

Sinclair (1974) developed a statistical method for analysing mineral deposits, but it has since then been applied to a wide range of data. After that, Chiodini et al. (1998) used the same approach to analyse $CO_2$ fluxes from soil diffuse degassing, conceiving the method today named GSA. In this approach, the data is plotted on a logarithmic probability plot where a single log-normal population plots as a straight line, while a more complex distribution (e.g., multi-modal distribution) plots as a curve with several of inflection points. The GSA consists of partitioning complex distributions into different log-normal populations and estimating the proportion, mean, and standard deviation of each population, following the graphical procedure by Sinclair (1974). The number of log-normal populations of a multi-modal distribution can be defined from the number of inflection points of the curve: *n* overlapping log-normal populations are characterised by a curve with *n* - 1 inflection points (Sinclair, 1974; Chiodini et al., 1998; Cardellini et al., 2003). The relative proportion between the combined population can be defined from the cumulative probability of the inflection points (Sinclair, 1974). Considering that the statistical parameters of the partitioned population refer to the logarithm of $CO_2$ flux, the estimated mean values of the $CO_2$ flux and its uncertainty were estimated by means of the Sichel's *t* estimator (David, 1977). Finally, the $CO_2$ output associated to each population is computed multiplying the mean value and the proportion of the population by the extent of the surveyed area (Chiodini et al., 1998).

While the GSA can be a valuable tool, it has some limitations as noted by Cardellini et al. (2003). These authors point out that the results obtained through GSA can be influenced by subjective choices, such as assuming a log-normal distribution for $\varphi CO_2$ when the true distribution may be more complex, and that the partitioning procedure can lead to multiple solutions.

To perform sGs, the *sgsim* algorithm developed by Deutsch and Journel (1998) was used in this study. The *sgsim* was run by using the WinGslib free toolbox of geostatistical software (available at http://www.statios.com/WinGslib). This approach generates multiple and equiprobable simulated spatial distributions of a variable of interest (i.e., realizations), based on a model of spatial correlation described by the variogram. The sGs method involves simulating values of a variable at each point in a grid, based on a Gaussian conditional cumulative distribution function defined on the basis of the experimental data. The multiple realizations are then post-processed to produce maps and to estimate the total $CO_2$ output and its uncertainty. For further details about this methodology, refer to Cardellini et al. (2003).

### 3.3 Isotopic composition of the diffuse $CO_2$ emission

To support the characterization of the source/es of the diffuse degassing, the isotopic composition of the $CO_2$ released by the soil was determined at six locations (Fig. 2-A) by collecting 12 gas samples using one of the portable fluxmeters adjusted for this purpose, according to the methodology described in Chiodini et al. (2008). Following Chiodini et al. (2008), we collected two samples of the gas inside the accumulation chamber at each measurement point. The fluxmeter was equipped with a valve in the gas line, placed just after the IR spectrometer, allowing the collection of the gas in the accumulation chamber during the $CO_2$ flux measurement (Fig. 2-B). Samples were collected with a syringe and injected into 12 ml vials with a pierceable butyl rubber septum (Exetainer®). The first sample was taken shortly after placing the chamber to allow for gas homogenization, while the second sample was collected later at a higher $CO_2$ concentration. The time interval between the first and second samples varied depending on the flux and was chosen to ensure a significant difference in concentration between the two samples. The isotopic composition of the diffuse $CO_2$ flux ($\delta^{13}C$-$CO_2$) was then computed using a mass balance equation (for more details, see Chiodini et al., 2008).

The analysis of the samples was conducted at the INGV-Naples (Osservatorio Vesuviano, Italy). $CO_2$ concentrations and carbon isotopic compositions were determined by coupling a gas chromatograph (Agilent Technologies 6890 N) with a continuous flow mass spectrometer (Finnigan Delta plus XP). The $CO_2$ concentration standard error is ± 5% and for the $\delta^{13}C$ is ±0.2‰.

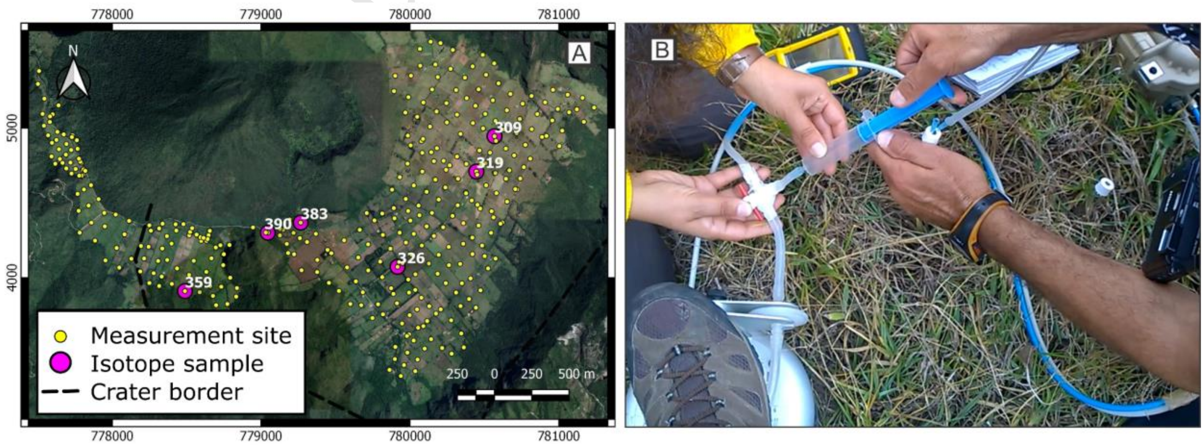


***Figure 2.*** *A.- Location of $CO_2$ flux and soil temperature measurement sites (small yellow dots) and sampling sites for carbon isotopes (large magenta dots).* ***B****.- Photograph of gas sampling for the carbon isotope determination.*

# 4 Results

## 4.1 $CO_2$ diffuse degassing

$CO_2$ fluxes ranged from ~2 to ~595 g $m^{-2}$ $d^{-1}$ (Supplementary Material 1). The measured φ$CO_2$ are reported in the logarithmic probability plot of Fig. 3 together with the results of the GSA analysis (Table1).

Upon modelling the statistical distribution, we identified several combinations of three log-normal populations that well reproduce the multimodal statistical distribution of the data set (Supplementary Material 2). Solutions including a complete, or even very strong overlap between the log-normal populations, suggesting an underlying factor that impedes the complete distinction and independence of these populations (Rice, 2007), were excluded.

The selected solution is reported in Fig. 3 that shows the good agreement of the model with the statistical distribution of the experimental data. The statistical parameters of the three populations of the selected model are reported in Table1.

Considering the statistical parameters of the partitioned populations and the extent of the surveyed area (3.36 $km^2$) the total $CO_2$ output is calculated by GSA approach, i.e., by summing the contribution of each population, is 154.2 t $d^{-1}$.

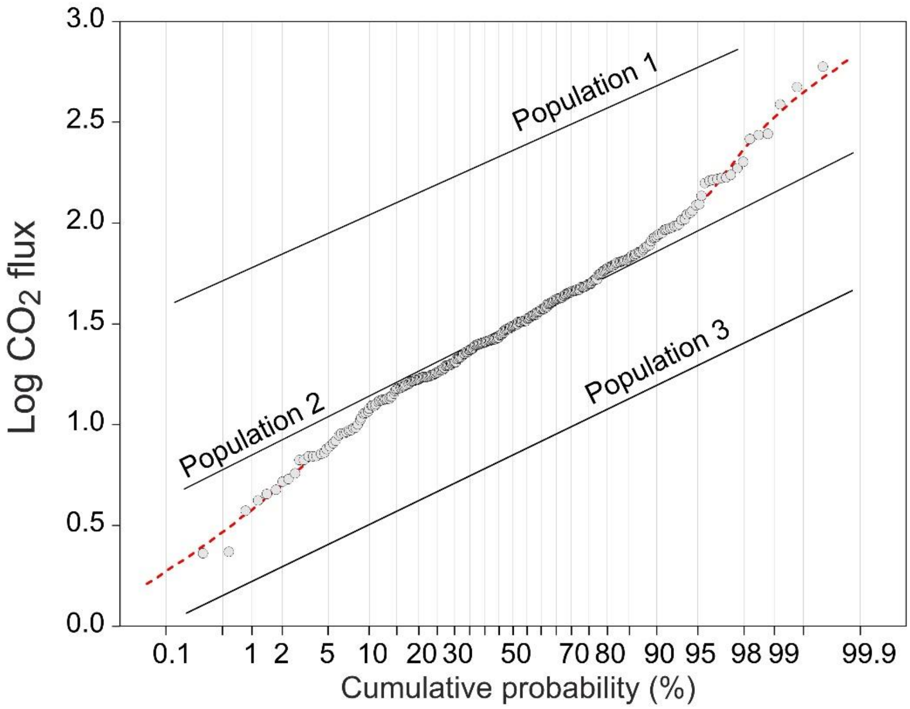

***Figure 3***.- *Probability plot of Log $\phi CO_2$ for Pululahua volcano and the result of the partition of the distribution into log-normal populations (straight lines). The red dashed curve represents the combination of the partitioned populations.*

***Table 1***.- *Estimated statistical parameters of the partitioned $CO_2$ flux populations.*

| **Population** | **Average log $CO_2$ flux** | **Standard deviation log $CO_2$ flux** | **%** | **Average $CO_2$ flux*** (g $m^{-2}$ $d^{-1}$) | **90% confidence interval of average $CO_2$ flux *** (g $m^{-2}$ $d^{-1}$) |
|---|---|---|---|---|---|
| Population 1 | 2.36 | 0.25 | 3.8 | 269.9 | 210.2 - 408.5 |
| Population 2 | 1.50 | 0.28 | 90.2 | 38.9 | 28.7 - 43.7 |
| Population 3 | 0.85 | 0.27 | 6.0 | 8.57 | 6.92 - 11.64 |

*Estimated by Sichel's t estimator method.

***Table 2***.- *Relevant parameters of sGs application.*

| **Parameter** | **Grid parameters** Cell size, number of cells in X, Y | **Variogram model** type, nugget, sill contribution, range |
|---|---|---|
| **$CO_2$ flux** | 10 m, 395, 260 | Spherical, 0.39, 0.6, 480 m |
| **Soil temperature** | | Spherical, 0.45, 0.56, 390 m |

The $\varphi CO_2$ map was obtained by applying the sGs algorithm, computing and modelling the experimental variogram of the normal scores of the flux data (Table 2 and Supplementary Material 3). The resulting map, reporting at each cell the average $\varphi CO_2$ from 200 simulations, is shown in Fig. 4-A. The sGs-computed total diffuse $CO_2$ output over the mapped area (3.36 $km^2$) is 126.2 ± 18.9 t $d^{-1}$.

Cardellini et al. (2003) evaluated how the number of measurements affects the uncertainty of estimating the total $CO_2$ output from volcanic and hydrothermal areas. They found that the total $CO_2$ output uncertainty is correlated with the combination of sampling density and range of spatial correlation of $\varphi CO_2$. By applying the empirical relation proposed by Cardellini et al. (2003), and considering the density of measurements in our survey and the range of the variogram of $\varphi CO_2$ (Table 2), an uncertainty of the estimation of the total $CO_2$ output of ~ 11% is obtained.

To further review the adequacy of our survey design, we randomly removed from the original dataset, which includes 350 measurements, 20% and 40% of the data to create two sub-datasets, one with 80% (n. = 280) and the other with 60% (n. = 210) of them. We then used these sub-datasets to create maps of soil $CO_2$ flux, that are compared to the map obtained with the entire dataset in Fig. S1 and S2 of Supplementary Material 4. The estimated diffuse total $CO_2$ output ranged from 126.2 t $d^{-1}$ for the 100% dataset as previously mentioned, to 131.1 t $d^{-1}$ and 132.1 t $d^{-1}$, respectively, for the 80% and 60% datasets. These variations were small (around 5-6 t $d^{-1}$), suggesting again that our sampling design can be considered robust to estimate the total $CO_2$ output.

### 4.2 $CO_2$ flux at “El Pailón”

The $CO_2$ flux values from the pool ranged from ~1,593 to ~29,595 g $m^{-2}$ $d^{-1}$ (Supplementary Material 1). A previous study reported an average $CO_2$ flux value of 389 g $m^{-2}$ $d^{-1}$ for several measurements from the pool surface (IG-EPN, 2016), which is significantly lower compared to our results. This variation could be attributed to the different location of the measuring points and possibly also due to diverse meteorological conditions during the two surveys. Summing up the $CO_2$ fluxes measured at the 17 sampled sites, which were uniformly distributed around the pool surface, we estimate a minimum emission of 3.6 kg $d^{-1}$ of $CO_2$ for the El Pailón pool.

Although the magnitude of this emission is negligible if compared to the amount of $CO_2$ released by soil diffuse degassing, the He isotopic composition of 2.72 $R/R_a$ (sample obtained during this survey; Ionescu, personal communication), provides an indication on the deep origin of the released gas.

Lages et al. (2021) and Inguaggiato et al. (2010) analysed noble gas isotope variation along the entire Andean Volcanic Arc and in the Ecuadorian volcanic arc, respectively. These authors state that in Ecuador, where the crust is approximately 50 km thick, volcanic $^3He/^4He$ ratios are around 7.4 R/Ra, which indicates crustal contamination by the addition of radiogenic crustal $^4He$ to magma as it ascends through this thick crust. Nevertheless, for the low temperature (<100 °C), peripheral gas emissions reported in their works (n = 28), we computed an average R/Ra of 2.9, closely matching the ratio measured in the current study at El Pailón. This can be explained by secondary processes such as the dilution of magmatic fluids by crustal helium, lowering the original $^3He/^4He$ ratio. Thus, we suggest that El Pailón pool reflects the typical helium isotopic composition of peripheral emissions from arc volcanoes in Ecuador, likely indicating a diluted magmatic helium signature due to the addition of atmospheric/crustal $^{4}He$.

### 4.3 Soil temperature

Soil temperatures were measured and found to range from 14.4°C to 31.8°C, with an average temperature of 20°C. Maximum air temperature was 24.4°C during the field activities. The soil temperature map was obtained by applying the sGs algorithm, computing and modelling the experimental variogram of the normal scores of the temperature data (Table 2 and Supplementary Material 3). The computation grid used is described in Table 2, and the resulting map is shown in Fig. 4-B.

Soil temperature and $\varphi CO_2$ are poorly correlated (Pearson's correlation coefficient between these two variables is near zero: -0.09). However, three distinct areas exhibit relatively higher temperature values (highlighted in orange in the map of Fig. 4-B).

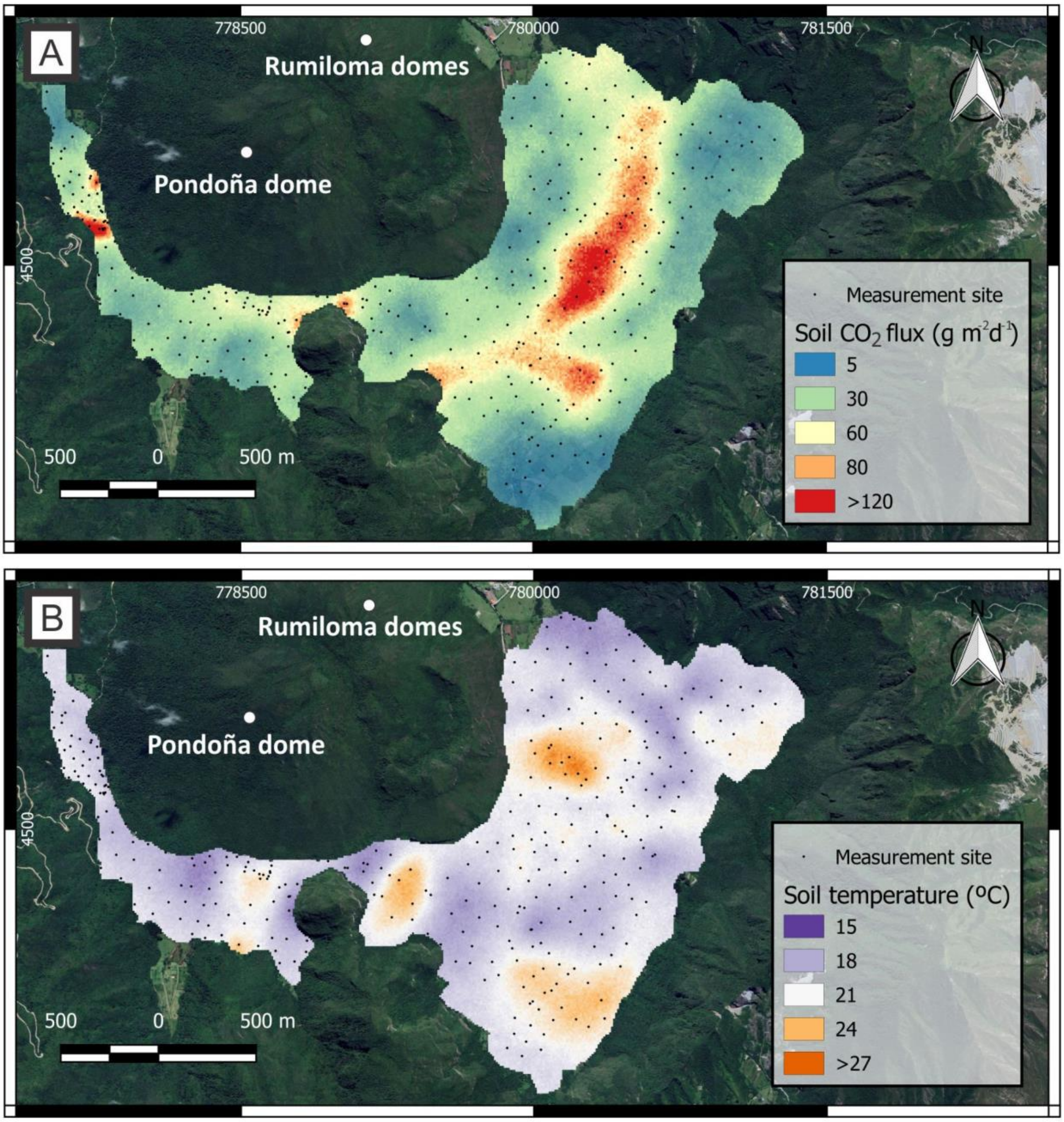


***Figure 4. A**.- Map of the $CO_2$ flux; **B**.- Map of soil temperature at Pululahua volcano. The maps report at each site the average of the parameter computed based in 200 simulations. Map coordinates are expressed in meters, WGS84 UTM 17N.*

### 4.4 Soil $CO_2$ carbon isotopic composition

We processed carbon isotopic data (Supplementary Material 5) following the approach proposed by Chiodini et al. (2008), to identify the different $CO_2$ sources and define the biogenic $CO_2$ background flux of the surveyed area. The computed $\delta^{13}C$ of the released $CO_2$ at the six investigated sites (Table 3) ranges from -10.45‰ to -3.45‰.

***Table 3**.- Computed isotopic composition of the $CO_2$ released by the soil and corresponding $CO_2$ flux.*

| Measuring point n. | $\delta^{13}C$ degassed $CO_2$ (‰ vs V-PDB) | Soil $CO_2$ flux ($g\ m^{-2}\ d^{-1}$) |
|---|---|---|
| 309 | -4.28 | 64.8 |
| 319 | -6.04 | 94.7 |
| 326 | -6.46 | 46.5 |
| 359 | -10.45 | 17.1 |
| 383 | -11.85 | 41.3 |
| 390 | -3.45 | 276.0 |

In Fig. 5, the computed isotopic compositions of the $CO_2$ released by soil degassing are compared with the theoretical values expected for the mixing between biogenic and isotopically heavier, i.e., volcanic $CO_2$ sources (e.g., Chiodini et al., 2008, Viveiros et al., 2010). For the biogenic source, the mixing lines were computed assuming: i) an isotopic composition of carbon of - 20‰, resulting from the average between the $\delta^{13}C$ for C3 plants ($\delta^{13}C$ = -27‰) and for C4 plants ($\delta^{13}C$ = -13‰) (Cheng, 1996), as we did not characterise in detail the local vegetation and assumed both types of organic contribution could be present, and ii) $CO_2$ fluxes of 4, 8.5 and 20 g $m^{-2}$ $d^{-1}$. For the possible volcanic-hydrothermal endmember, because there are no fumaroles in the area, we considered the $\delta^{13}C$ of the largest $CO_2$ flux characterised for the isotopic composition (-3.45‰; Table 3). This value is compatible with the isotopic composition of four different samples of crater fumaroles of Guagua Pichincha volcano, an arc volcano located 27 km to the Southwest of Pululahua, collected during the same Volcanic Gas Workshop in which we carried out this work, which ranges from -4.9‰ to -3.43‰ (average of -4.1‰; Sierra, 2022).

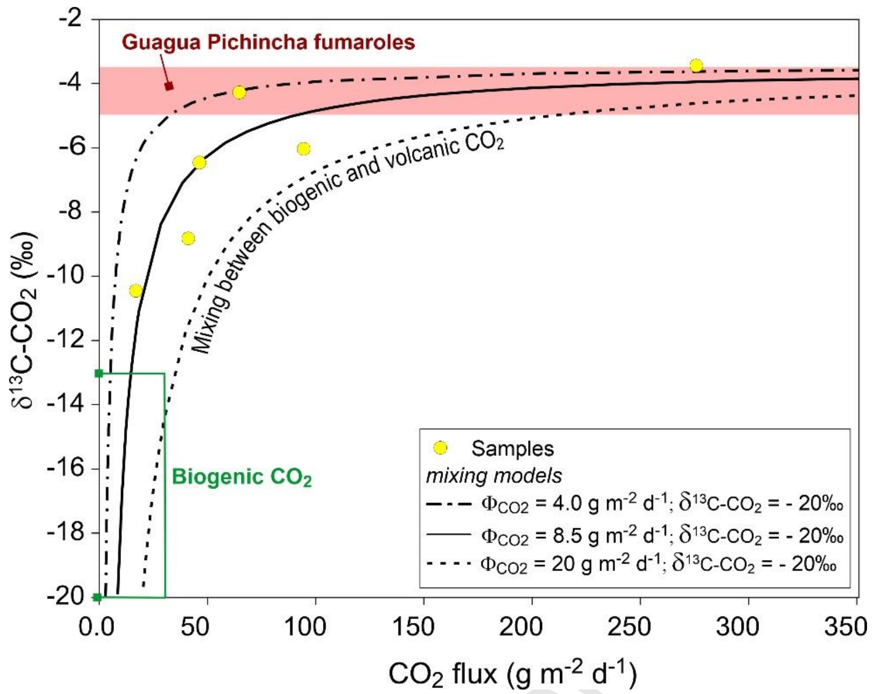


***Figure 5**.- Carbon isotopic composition of soil $CO_2$ efflux vs soil $CO_2$ flux. $\delta^{13}C$-$CO_2$, is expressed as ‰ vs. V-PDB. The ranges of isotopic compositions of biogenic $CO_2$ (Cheng et al., 1996) and of Guagua Pichincha fumaroles (Sierra, 2022), and three theoretical mixing lines between biogenic and volcanic fluxes are shown. The mixing was computed considering an average $\delta^{13}C$-$CO_2$ = -20‰ for the biogenic endmember and three $\phi CO_2$ values for the potential biological flux (4, 8.5, and 20 g $m^{-2}$ $d^{-1}$), and a $\delta^{13}C$-$CO_2$ = -3.45 ‰ for the volcanic endmember. See text for explanation.*

## 5 Discussion

Soil $CO_2$ fluxes, soil temperature and isotopic composition of the released $CO_2$ are discussed to characterise the diffuse degassing around the youngest intra-crater domes of Pululahua volcano (Pondoña and Rumiloma I and II), to define the occurrence of a diffuse degassing structure and to quantify the emission of volcanic $CO_2$. Finally, considerations about the hazard related to $CO_2$ degassing are also addressed.

### 5.1 Sources of $CO_2$ and diffuse degassing structures

In this section, we discuss our approach to characterise the sources of diffuse degassing and the occurrence of a diffuse degassing structures at Pululahua Dome Complex. Diffuse degassing structures (DDS, Chiodini et al., 2001) are the areas releasing volcanic $CO_2$. Statistical analysis of $\varphi CO_2$ (section 4.1) resulted in three log-normal populations (Fig. 3, Table 1), Population 1 (P1) is high (~270 g $m^{-2}$ $d^{-1}$), Population 2 (P2) is intermediate (39 g $m^{-2}$ $d^{-1}$), and Population 3 (P3) is low (8.5 g $m^{-2}$ $d^{-1}$) average $\varphi CO_2$, respectively. High soil $CO_2$ flux populations, i.e., fluxes higher than hundreds of g m$^{-2}$ d$^{-1}$, are commonly indicative of a volcanic, or more in general of a geogenic, origin for $CO_2$ emissions. Lower flux populations, characterised by fluxes from few grams to tens of g m$^{-2}$ d$^{-1}$, are instead generally associated to a biogenic source of $CO_2$, being these values in the range of fluxes reported in the literature for the biologic activity in the soil (e.g., Raich and Schlesinger; 1992; Norman et al., 1992; Bajracharya et al., 2000; Raich and Tufekcioglu, 2000; Nakadai et al., 2002). Furthermore, in order to define a threshold flux above which $\varphi CO_2$ can be considered to have a volcanic contribution, a frequently used approach is to use the 95$^{th}$ cumulative probability of flux population attributed to the biogenic source (e.g., Viveiros et al., 2010; 2020).

The interpretation of the $CO_2$ source of intermediate fluxes (i.e., of tens up to hundred g m$^{-2}$ d$^{-1}$) only on the basis of the magnitude of the flux, can be more challenging because, for example: i) the presence of both poorly and strongly vegetated soil in the same area can result in the coexistence of low and intermediate flux populations; ii) seasonal variation of the biologic activity can produce strong variations in the $CO_2$ flux from the soil; iii) low levels of deeply produced $CO_2$ degassing can result in fluxes of the same order of magnitude of the biologic~~al~~ one. In addition, intermediate flux populations, or even low flux populations, were interpreted in several studies as representative of a mixed contribution from both volcanic and biogenic sources (e.g., Chiodini et al., 2008; 2015; Viveiros et al., 2010; 2020; Bini et al., 2019; Di Martino et al., 2020, among others).

At Pululahua, P3 can be reasonably associated to the biologic activity on the basis of its average flux and considering that its 95$^{th}$ percentile is ~20 g m$^{-2}$ d$^{-1}$. At the same time, P1, representative of high $CO_2$ fluxes (average of ~270 g m$^{-2}$ d$^{-1}$ and 95$^{th}$ percentile of ~590 g m$^{-2}$ d$^{-1}$), can be associated with the degassing of volcanic $CO_2$. And P2, even if it is characterised by a relatively low average flux (~39 g m$^{-2}$ d$^{-1}$), theoretically possible for the biogenic source, shows a quite high 95$^{th}$ percentile of ~90 g m$^{-2}$ d$^{-1}$. In addition, the C-isotope data of $CO_2$ released by the soil show fluxes in the range from ~40 g m$^{-2}$ d$^{-1}$ to 65 g m$^{-2}$ d$^{-1}$ (Table 3) with an isotopic composition ranging from -8.83‰ to -4.28‰, suggesting a mixture between, the here considered, biologic (-20 ‰) and the volcanic (-3.45‰) $CO_2$ endmembers. This suggests that P2 cannot univocally be associate to a pure biological source different from that feeding P1 (e.g., to areas with more dense vegetation respect to those represented by P3) nor to areas of weak, but purely, volcanic degassing. In other words, P2 most likely represents a combination of biologic and volcanic $\varphi CO_2$. Unfortunately, the relatively low number of isotopic data of the degassed $CO_2$ does not allow a more in-depth analysis.

The spatial distribution of fluxes in the surveyed area highlights a clear radial pattern, with the highest $\varphi CO_2$ values concentrated around the perimeters of the young domes (fluxes in red in Fig. 4A). This pattern underscores the presence of elevated diffuse $CO_2$ degassing enveloping the impermeable structure of the domes. This suggests that the young, central domes in the caldera act as a barrier to fluid ascent, forcing $CO_2$ to reach the surface along the contact between the impermeable domes and the more permeable volcanic block-and-ash deposits that makes up the Pululahua crater floor. It is worth noting that, as it was mentioned in section 3.1, we did not survey the domes, hence our assumption of the low permeability of the domes is based in previous works performed in similar geologic scenarios. Lava domes' geomorphic control over $CO_2$ degassing has been reported in other degassing areas around the world, such as Cuicocha Volcanic Complex, in Ecuador (Sierra et al., 2020), around the dome of Showa-Shinzan volcano, in Japan (Hernández et al., 2006), in Rotorua geothermal system, in New Zealand (Werner and Cardellini, 2006), or at Furnas volcano, in Portugal (Viveiros et al., 2010).

### 5.2 Volcanic $CO_2$ output

The total $CO_2$ output by diffuse degassing was estimated using two different approaches, GSA and sGs, resulting in 154 t $d^{-1}$ and 126 t $d^{-1}$, respectively. Since this amount includes both the biogenic and volcanic sourced $CO_2$, to estimate the volcanic $CO_2$ emission of the Pululahua it is necessary to exclude the biologic contribution. Due to the uncertainties discussed in the previous section, we cannot apply in a straight way the GSA approach, consisting in the computation of the output associated to each $\varphi CO_2$ population, mainly because P2 represents a mixture of biologic and volcanic $CO_2$.

For this reason, and because it is discussed in the literature that $CO_2$ output estimation based on the results of the sGs can be considered more reliable than those obtained with the GSA, especially because GSA does not consider the spatial structure of the data (e.g., Cardellini et al., 2003; Frondini et al., 2004; Lewicki et al., 2005; Viveiros et al., 2020), we attempted to quantify the volcanic $CO_2$ emission by subtracting to the sGs estimated total $CO_2$ output the biologic contribution, which was computed assuming a "typical biological flux" constant over the entire mapped area (Chiodini et al., 2007; Viveiros et al., 2010; Chiodini et al., 2020; 2021; Li Vigni et al., 2022).

The "typical biological flux" was estimated following two approaches, leading to two different estimates of the volcanic $CO_2$ emission:

1) Considering the average $\phi CO_2$ of P3 (8.5 g $m^{-2}$ $d^{-1}$) as the "typical biological flux", given that P3 population can be clearly associated to a biogenic source and this value allows to explain some of the available isotopic data shown in Fig. 5. This results in estimated biogenic and volcanic contributions of ~ 29 t $d^{-1}$ and 97 t $d^{-1}$, respectively. Probably, this assumption slightly overestimates

the volcanic emission, considering that it is not possible to fully characterise biological fluxes with the available data (see section 5.1).

2) Considering as the "typical biological flux" a $\phi CO_2$ of 20 g $m^{-2}$ $d^{-1}$, which: i) represents the $95^{th}$ cumulative percentile of P3, i.e., an upper limit for the only flux population that can be clearly associated to the biogenic source, ii) agrees with a possible upper limit flux of the mixing models reported in Fig. 5, and iii) it is a value similar to those found for the biogenic background in other surveys of volcanic-hydrothermal areas (Chiodini et al., 2008, 2015; Viveiros et al., 2010). With this assumption biogenic and volcanic contributions result in ~67 t $d^{-1}$ and 59 t $d^{-1}$, respectively.

The volcanic $CO_2$ contribution of the whole system likely lies between 97 t $d^{-1}$ and 59 t $d^{-1}$, depending on our definition of the "typical biological flux": the average $\phi CO_2$ or the $95^{th}$ cumulative percentile of P3.

Our estimation of the total $CO_2$ output (~126 t $d^{-1}$) shows a stark difference compared to a previous study of the Pululahua Dome Complex performed by Padrón et al. (2008), who reported a $CO_2$ emission of 270 t $d^{-1}$. This difference could result from the different extent of the surveyed areas and the different sample spacing. While our sampling pattern was quite regular and detailed (i.e., 350 $CO_2$ flux measurements over an area of 3.36 $km^2$ around Pondoña and Rumiloma domes), Padrón et al. (2008) used a more irregular sampling pattern, including 217 $\phi CO_2$ measurements over a much larger area of 27.6 $km^2$ that extended beyond Pululahua's crater.

To try to assess how Padrón et al. (2008) survey design affected the uncertainty of the $CO_2$ output at Pululaha we applied the empirical relationship from Cardellini et al. (2003) (used above in section 4.1). Considering the extent of the surveyed area (27.6 $km^2$) and the number of measurements (217) from Padrón et al. (2008), combined with the spatial features of the $CO_2$ flux resulting from our survey (i.e., the range of the $CO_2$ flux variogram of 480 m), the empirical relation proposed by Cardellini et al. (2003) indicates an uncertainty of about 46% for the total $CO_2$ output estimate. This suggests that the spacing between the measurements of Padrón et al. (2008) did not allow capturing the actual spatial structure of the $CO_2$ flux, possibly leading to an overestimation of the $CO_2$ emission.

Normalizing the two total $CO_2$ outputs for the investigated area, Padrón et al. (2008) estimation suggests an emission rate of ~9.8 t $d^{-1}$ $km^{-1}$, while our data suggest 37.5 t $d^{-1}$ $km^{-1}$. We believe this substantial difference does not reflect an increase in Pululahua degassing between 2008-2017, but rather stems from discrepancies in the estimation of the $CO_2$ emission due to the sampling pattern and methodologies employed. Padrón et al. (2008) based their estimation on a wide area with sparse sampling points, encompassing regions we consider to have low permeability, such as the domes. Moreover, they included 'synthetic points' to complete the sampling pattern in inaccessible zones, whereas our focus was on the crater basin, which shows notably higher permeability.

Despite disparities in estimations and differences in the sampled areas, the distribution of the $CO_2$ emitted around the young domes of the Pululahua Dome Complex in both studies show significant agreement.

### 5.3 Soil temperature

The spatial distribution of soil temperature at Pululahua shows a different pattern when compared to $\varphi CO_2$, contrary to what is commonly observed in numerous volcanic-hydrothermal diffuse degassing areas where $CO_2$ degassing is associated to relatively shallow condensation of the steam that heats the soil (e.g., Viveiros et al., 2010; 2020; Melián et al., 2012; Cardellini et al., 2017; Bini et al., 2019; Lamberti et al., 2019; Chiodini et al., 2021). The ambient temperature strongly influences soil temperature, as evidenced by a correlation coefficient of 0.94. The highest soil temperature measurements were roughly 5°C higher than maximum ambient temperature (which was 24.4 °C on the days of our survey). These observations are probably justified by the insolation effect that resulted in higher temperature measurements where the soils are exposed (Blank et al., 2002), thus not allowing to consider the recorded soil temperatures as “anomalous”, i.e., as associated with uprising hot fluids from the hydrothermal system.

In order to investigate the relatively high values of soil temperature registered, on October 12$^{th}$, 2023, IG-EPN members conducted a new exploratory temperature measurement campaign in the Pululahua crater basin to confirm, or not, the presence of the soil temperature anomalies. In this second survey, the highest temperature values highlighted by Fig. 4 B were not detected: 46 measurements ranged between 17.3°C and 22.6°C, with an average of 20.2°C and a standard deviation of 1.3. This indicates the absence of deep origin for the soil temperature anomalies and therefore, suggesting that the soil temperature variations seem to be controlled by the types of soil and the effects of the sun radiation.

The presence of cold diffuse $CO_2$ emissions in volcanic systems can result from multiple causes. For example, slow gas transport or a deep gas source, distant from the surface, can cause a complete steam condensation deep in the ground, with no detectable heat anomaly at the surface (Giammanco et al., 2016). Furthermore, significant variations in temperature between the surface and the subsurface may also exist due to factors such as heat flow, hydrothermal circulation, and groundwater movement (Ingebritsen and Ziagos, 1995).

### 5.4 $CO_2$ emissions and associated hazards

$CO_2$ is among the most abundant species in volcanic gases and it is usually diluted by the air when it is released from the soil. However, since this gas is 1.5 times heavier than air (at standard pressure and temperature conditions), at cold gas emission areas it can flow over the soil and accumulate in topographic depressions (e.g. Le Guern et al., 1982; Chiodini et al., 2010; Edmonds et al., 2015; IVHHN, 2016; USGS, 2016). High concentrations of $CO_2$ are hazardous, as they reduce oxygen leading to health risks. Inhaling air with more than 3% of $CO_2$ can quickly cause headaches, dizziness, increased heart rate, and shortness of breath. Concentrations of $CO_2$ greater than 15% rapidly result in unconsciousness, with severe consequences (e.g., NIOSH, 1981; Blong, 1984; Baxter et al., 1999; Schlesinger and Cassee, 2003).

Increasingly, volcanologists worldwide have begun to recognize volcanic gas emissions, including $CO_2$, as relevant hazards (Farrar et al., 1995; Baxter et al., 1999; Hansell and Oppenheimer, 2004; Viveiros et al., 2009; 2016; Smets et al., 2010; Andrade et al., 2012; Auker et al., 2013; Mazot et al., 2013; Edmonds et al., 2015; Williams-Jones and Rymer, 2015; Balagizi et al., 2018; Venturi et al., 2019; Melián et al., 2021; Di Martino et al., 2022).Tragedies, such as six fatalities due to $CO_2$ inhalation in a small thermal spa of Tangalí, located ~30 km north of Pululahua, in January 2015, are a reminder of the hazard that volcanic gases can pose during quiescent periods of activity, also in Ecuador (Benalcazar, 2015; Sierra et al., 2020; Melián et al., 2021).

Narratives from Pululahua report the death of small animals and even young livestock in topographic depressions and caves (IG-EPN, 2016; Fig. 6-A). $CO_2$ fluxes >65,000 g $m^{-2}$ $d^{-1}$ were measured in a specific cavern located in the southwestern border of the Pondoña dome (Pillahuas zone; point 2 in Fig. 6) (IG-EPN, 2016). Fortunately, to date, no human losses have been reported in the study area. However, hazards associated with ~~soil~~ $CO_2$ diffuse degassing at Pululahua need to be evaluated because: (1) of fatalities of small and large animals, (2) the surveyed area is home to approximately 50 families, who use it for agriculture and/or touristic purposes (Andrade et al., 2012), and (3) the Geobotanical Reserve that receives thousands of national and international tourists annually. In addition to these factors mainly related with the exposure, it is essential to consider that diffuse $\varphi CO_2$ at Pululahua is emitted through cold soils that may result in the accumulation of high $CO_2$ close to the soil, especially in depressions and poorly ventilated zones (Viveiros et al., 2009; 2016). Emissions are even more “silent” since hot soils can provide direct evidence of the presence of volcanic fluids in the area. Eventual depressions should be identified in the area and any ~~further~~ action that includes excavations should consider the potential risk of $CO_2$ accumulation in the identified DDS zones.

Our detailed $\varphi CO_2$ map constitutes additional information for Puluahua's volcanic hazard map (Hall et al., 1988; Vasconez, 2019), which provides an appropriate visualization of the soil $CO_2$ emissions. Fig. 6-B shows a map that represents the probability of the simulated fluxes at each location to exceed the value of 40 g $m^{-2}$ $d^{-1}$, which, according to our isotopic data and to the GSA analysis, may represent, for the study area, a reasonable value for the occurrence of even low volcanic $CO_2$ contribution. In other words, this map highlights the areas affected by degassing of volcanic $CO_2$ (DDS). It is noteworthy that the location of the depressions where dead animals have been found are included in the DDS.

Over the last decade, several researchers have focused on case studies that have highlighted a previously overlooked volcanic hazard: the indoor accumulation of hazardous concentrations of $CO_2$ in villages located on top of diffuse degassing areas (Viveiros et al., 2015; 2016; Venturi et al., 2019; Lamberti et al., 2021; Gurrieri et al., 2023). Although $\varphi CO_2$ measured in Pululahua currently remains relatively low across most of the crater basin, monitoring indoor $CO_2$ concentrations could effectively prevent future potential issues, especially in case of a volcanic unrest. Additionally, for the very few buildings already emplaced, it might be recommendable to pay special attention in keeping the rooms ventilated and, if possible, to impermeabilize the ground floor to avoid gas infiltration. This type of recommendations should be potentially included in the building codes focused on populations settled on top of volcanic degassing areas worldwide. Because of our results, we believe that the map presented in Fig. 6 could be a useful tool for land use planning. Future studies should include not only evaluation of indoor $CO_2$ concentrations, but also assess the physical vulnerability of the buildings, such as existence of basements, existence of permeable membranes and/or ventilation systems.

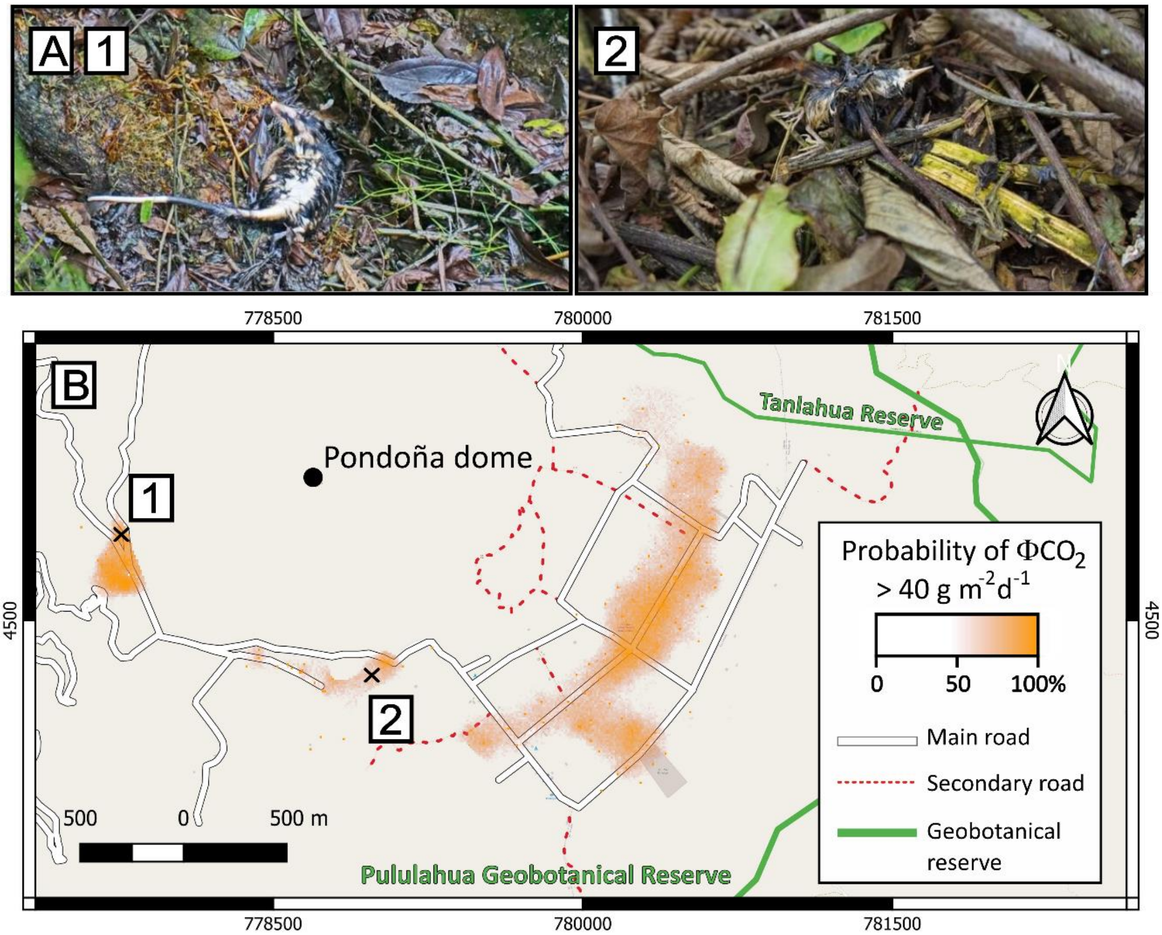


*__Figure 6__. __A__.- 1 and 2. Small animal corpses (opossum and bird) found in the $CO_2$ source zones, which suggest death by suffocation when exposed to the released $CO_2$ (Photos: FJ. Vasconez). __B__.- Probability map of $CO_2$ flux exceeding 40 g $m^{-2}$ $d^{-1}$ threshold selected to discriminate volcanic-hydrothermal soil $CO_2$ degassing (i.e. > 40 g $m^{-2}$ $d^{-1}$). The two black crosses in the map mark the position in which both corpses were found (1 and 2). The base map is sourced from OpenStreetMap.*

## 6 Concluding remarks

This work represents the collaborative efforts of an international group of researchers during the CCVG-IAVCEI 13th Gas Workshop held in Ecuador aimed at applying recognized and well-established methodologies to collect and analyse $CO_2$ flux and temperature data.

Pululahua, an active dome complex near Quito, the capital city of Ecuador, serves as a popular tourist attraction and is inhabited by several small communities. Given the current population and significant tourist influx in this area, it is imperative to gain a thorough understanding of $CO_2$ emissions within the area as well as to monitor the state of the volcanic system.

Our survey aimed to produce a comprehensive map of $CO_2$ emissions specifically in the Pululahua crater floor. By using established methods of data analysis, we were able to provide a more robust estimation of $CO_2$ emissions compared to the existing one, as well as to provide, for the first time, some constrain on the volcanic $CO_2$ emissions at Pululahua based also on carbon isotopes data.

The $CO_2$ flux map showed anomalous values enveloping the domes, suggesting a significant control of the dome permeability on the gas transfer toward the surface. Soil temperature and $CO_2$ flux data were poorly correlated, and the higher temperatures measured are probably explained by the soil exposure and insolation.

We observed that in this case, where the biogenic and mixed volcanic-biogenic fluxes appear to be of similar magnitude, the GSA method could not effectively discriminate the sources of soil $CO_2$ degassing. For this reason, it was not possible with this method to define a reliable threshold for biogenic $CO_2$ flux, a parameter that is frequently used to define the spatial extent of the DDS.

To distinguish between volcanic, mixed, and biogenic sourced of $\varphi CO_2$ more accurately, we recognize the need for extensive soil $CO_2$ sampling across our study area and a comprehensive analysis of $\delta^{13}C\text{-}CO_2$. This study highlights the need to complement diffuse degassing studies with carbon isotopic data in order to discriminate between the different sources of $CO_2$, and provide a deeper understanding of the complex processes underlying the origin and release of diffuse $CO_2$, which should be considered in future works and in other case studies.

This work allowed us to update the estimations of the carbon budget of the Pululahua volcanic Dome Complex and to provide for the first time an estimate of the volcanic $CO_2$ emissions, ranging from 59 to 97 t $d^{-1}$ from diffuse degassing. This estimation can be included in the MaGa database, a collaborative project aimed at gathering data on gas emissions from geological systems (http://www.magadb.net/), contributing to the efforts for the quantification of the Earth carbon budget.

This study can be considered as a baseline for future investigations in Pululahua. Carrying out new campaigns in the area preserving a similar approach would be helpful to detect temporal and/or seasonal variations in the area and is crucial for a volcano monitoring programme.

**STATEMENT**

The authors have no competing interests to declare.

**Acknowledgments**

We appreciate the comments made by reviewers Cynthia Werner and an anonymous reviewer, which substantially helped improve the content of the manuscript. The authors would like to thank the organizing committee of the CCVG 13th Gas Workshop. This paper is Contribution No. R-487 of the IDEAN - Instituto de Estudios Andinos Don Pablo Groeber. MCL would like to acknowledge funding that supported her attendance to the workshop from the University of Buenos Aires (UBACyT 20020150200230BA). The IG-EPN research group, DS, FV, and SH wish to acknowledge the project "Generación de capacidades para la emisión de alertas tempranas-SENPLADES" and to their research projects obtained by the IG-EPN though SENESCYT and BID. CC wishes to acknowledge for the financial support Deep Carbon Observatory (DCO) Grant n. PO62355 and Italian Ministry of Ministry of University and Research (MUR) project PRIN2022-2022HA8XCS “CRUSCA”. FV and CS wish to thank the Portuguese FCT funding agency (Ref. FCT UIDP/00643/2020, DOI 10.54499/UIDP/00643/2020). B.M.K wishes to acknowledge for the Research grant SRG-UBB33023/26.06.2023 by Babes-Bolyai University, Romania.

**Author contributions**

**Lamberti**, M.C.: Conceptualization; Acquisition of data in the field; Data curation; Formal analysis; Writing - original draft; Review & editing.

**Sierra**, D.: Conceptualization; Acquisition of data in the field; Data curation; Formal analysis; Writing - original draft; Review & editing.

**Cardellini**, C.: Conceptualization; Acquisition of data in the field; Data curation; Formal analysis; Writing - original draft; Review & editing.

**Viveiros**, F.: Conceptualization; Acquisition of data in the field; Data curation; Formal analysis; Writing - original draft; Review & editing.

**Vásconez Müller**, A.: Acquisition of data in the field; Writing - review & editing.

**Vasconez**, F.J.: Acquisition of data in the field; Writing - review & editing.

**Narváez**, D.F.: Acquisition of data in the field; Writing - review & editing.

**Silva**, C.: Acquisition of data in the field; Data curation; Formal analysis; Review & editing.

**Melián**, G.: Acquisition of data in the field; Data curation; Formal analysis; Review & editing.

**Caliro**, S.: Analysis of isotopic data in the laboratory.

**Kis**, B.M.: Acquisition of data in the field; Data curation; Formal analysis; Review & editing.

**Ionescu**, A.: Acquisition of data in the field; Data curation; Formal analysis; Review & editing.

**Hidalgo**, S.: Conceptualization.

**References**

Alvarado, A., Audin, L., Nocquet, J.M., Lagreulet, S., Segovia, M., Font, Y., Lamarque, G., Yepes, H., Mothes, P., Rolandone, F., Jarrín, P., & Quidelleur, X. 2014. Active tectonics in Quito, Ecuador, assessed by geomorphological studies, GPS 580 data, and crustal seismicity. Tectonics 33, 67–83. https://doi.org/10.1002/2012TC003224

Amundson, R., Stern, L., Baisden, T., & Wang, Y. 1998. The isotopic composition of soil and soil respired $CO_2$. Geoderma 82: 83 – 114. https://doi.org/10.1016/S0016-7061(97)00098-0

Andrade, C., Cruz, J.V., Viveiros, F., & Coutinho, R. 2020. $CO_2$ emissions from Fogo intracaldera volcanic lakes (São Miguel Island, Açores): a tool for volcanic monitoring. Journal of Volcanology and Geothermal Research, 400, 106915. doi: https://doi.org/10.1016/j.jvolgeores.2020.106915

Andrade, C., Viveiros, F., Cruz, J.V., Branco, R., Moreno, L., Silva, C., Coutinho, R., & Pacheco. J.E. 2019. Diffuse $CO_2$ flux emission in two maar crater lakes from São Miguel (Azores, Portugal). Journal of Volcanology and Geothermal Research, 369: 188-202, doi: doi.org/10.1016/j.jvolgeores.2018.11.030

Andrade, D., Hidalgo, S., Monzier, M., Eissen, J., & Beate, B. 2012. Serie Los Peligros Volcanicos Asociados con el Atacazo Ninahuilca y Puluhua. Series Volcanic Hazards Associated with the Ninahuilca and Puluhua. Corporación Nacional del Ecuador IG-EPN, IRD, 112 pp.

Andrade, S. D., Müller, A. V., Vasconez, F. J., Beate, B., Aguilar, J., & Santamaría, S. 2021. Pululahua dome complex, Ecuador: eruptive history, total magma output and potential hazards. Journal of South American Earth Sciences, 106. https://doi.org/10.1016/j.jsames.2020.103046

Auker, M. R., Sparks, R. S. J., Siebert, L., Crosweller, H. S., & Ewert, J. 2013. A statistical analysis of the global historical volcanic fatalities record. Journal of Applied Volcanology, 2(1), 1-24. https://doi.org/10.1186/2191-5040-2-2

Balagizi, C. M., Kies, A., Kasereka, M. M., Tedesco, D., Yalire, M. M., & McCausland, W. A. 2018. Natural hazards in Goma and the surrounding villages, East African Rift System. Natural Hazards, 1-36. https://doi.org/10.1007/s11069-018-3288-x

Barberi, F., Coltelli, M., Ferrara, G., Innocenti, F., Navarro, J.M., & Santacroce, R. 1988. Plio-Quaternary volcanism in Ecuador. Geol. Mag. 125, 1–14. https://doi.org/10.1017/S0016756800009328

Baxter, P. J., Baubron, J. C., & Coutinho, R. 1999. Health hazards and disaster potential of ground gas emissions at Furnas volcano, Sao Miguel, Azores. Journal of Volcanology and Geothermal Research, 92(1-2), 95-106. https://doi.org/10.1016/S0377-0273(99)00070-0

Bernard, B. & Andrade, D. 2011. Volcanes cuaternarios del Ecuador Continental. Quaternary volcanoes of Continental Ecuador. Quito: IG-EPN/IRD.

Bini, G., Chiodini, G., Cardellini, C., Vougioukalakis, G. E. & Bachmann, O. 2019. Diffuse emission of CO2 and convective heat release at Nisyros caldera (Greece). Journal of Volcanology and Geothermal Research 376: 44-53. https://doi.org/10.1016/j.jvolgeores.2019.03.017

Blank, R. R., Welp, L. J., & Young, J. M. 2002. Soil temperature variability on a mountainside in the Alaskan taiga. Arctic, Antarctic, and Alpine Research 34 (2): 192-200.

Blong, R. J. 1984. Volcanic hazards: a sourcebook on the effects of eruptions. Elsevier. https://doi.org/10.1016/C2009-0-21853-8.

Bourdon, E., Eissen, J. P., Gutscher, M. A., Monzier, M., Hall, M. L., & Cotten, J. 2003. Magmatic response to early aseismic ridge subduction: the Ecuadorian margin case (South America). Earth and Planetary Science Letters, 205 (3-4): 123-138. https://doi.org/10.1016/S0012-821X(02)01024-5

Carapezza, M.L. & Federico, C. 2000. The contribution of fluid geochemistry to the volcano monitoring of Stromboli. Journal of Volcanology and Geothermal Research 95(1-4):227-245. doi: 10.1016/S0377-0273(99)00128-6

Cardellini, C., Chiodini, & G., Frondini, F. 2003. Application of stochastic simulation to $CO_2$ flux from soil: mapping and quantification of gas release. Journal of Geophysical Research 108. 2425 https://doi.org/10.1029/2002JB002165

Cardellini, C., Chiodini, G., Frondini, F., Avino, R., Bagnato, E., Caliro, S., Lelli, M., & Rosiello, A. 2017. Monitoring diffuse volcanic degassing during volcanic unrests: The case of Campi Flegrei (Italy). 2017. Scientific Reports 7, 6757. https://doi.org/10.1038/s41598-017-06941-2

Cerón, C. 2004. Reserva Geobotánica del Pululahua, Formaciones Vegetales, diversidad, endemismo y vegetación. Pululahua Geobotanical Reserve, Plant Formations, diversity, endemism and vegetation. Revista Cinchonia (5), Escuela de Biología, Universidad Central del Ecuador. Editorial Universitaria, Quito, 108 pp.

Cheng, W. 1996. Measurement of rhizosphere respiration and organic matter decomposition using natural 13C, Plant and Soil, 183, 263–268.

Chiodini, G. & Frondini, F. 2001. Carbon dioxide degassing from the Albani Hills volcanic region, Central Italy. Chemical Geology, 177(1-2), 67-83.

Chiodini, G., Baldini, A., Barberi, F., Carapezza, M.L., Cardellini, C., Frondini, F., Granieri, D., & Ranaldi, M. 2007. Carbon dioxide degassing at Latera caldera (Italy): Evidence of geothermal reservoir and evaluation of its potential energy. Journal of Geophysical Research Solid Earth 112. https://doi.org/10.1029/2006JB004896

Chiodini, G., Caliro, S., Cardellini, C., Avino, R., Granieri, D., & Schmidt A. 2008. Carbon isotopic composition of soil $CO_2$ efflux, a powerful method to discriminate different sources feeding soil $CO_2$ degassing in volcanic-hydrothermal areas. Earth and Planetary Science Letters, 274. https://doi.org/10.1016/j.epsl.2008.07.051

Chiodini, G., Cardellini, C., Bini, G., Frondini, F., Caliro, S., Ricci, L., & Lucidi, B. 2021. The Carbon Dioxide Emission as Indicator of the Geothermal Heat Flow: Review of Local and Regional Applications with a Special Focus on Italy. Energies 14, 6590. https://doi.org/10.3390/en14206590

Chiodini, G., Cardellini, C., Caliro, S., Avino, R., Donnini, M., Granieri, D., Morgantini, N., Sorrenti, D., & Frondini, F. 2020. The hydrothermal system of Bagni San Filippo (Italy): fluids circulation and $CO_2$ degassing. Italian Journal of Geosciences 139. https://doi.org/10.3301/IJG.2020.12

Chiodini, G., Cioni, R., Guidi, M., Marini, L., & Raco, B. 1998. Soil $CO_2$ measurements in volcanic and geothermal areas. Applied Geochemistry 13. https://doi.org/10.1016/S0883-2927(97)00076-0

Chiodini, G., Frondini, F., Cardellini, C., Granieri, D., Marini, L., & Ventura, G. 2001. $CO_2$ degassing and energy release at Solfatara volcano, Campi Flegrei, Italy. Journal of Geophysical Research: Solid Earth 106. http://dx.doi.org/10.1029/2001JB000246

Chiodini, G., Frondini, F., Kerrick, D. M., Rogie, J., Parello, F., Peruzzi, L., & Zanzari, A. R. 1999. Quantification of deep $CO_2$ fluxes from Central Italy. Examples of carbon balance for regional aquifers and of soil diffuse degassing. Chemical Geology, 159, 205-222.

Chiodini, G., Granieri, D., Avino, R., Caliro, S., Costa, A., Minopoli, C., & Vilardo G. 2010. Non-volcanic $CO_2$ Earth degassing: Case of Mefite d'Ansanto (southern Apennines), Italy, Geophysical Research Letters 37. https://doi.org/10.1029/2010GL042858

Chiodini, G., Granieri, D., Avino, R., Caliro, S., Costa, A., & Werner, C., 2005. Carbon dioxide diffuse degassing and estimation of heat release from volcanic and hydrothermal systems. Journal of Geophysical Research: Solid Earth 110. http://dx.doi.org/10.1029/2004JB003542

David, M. 1977. Geostatistical Ore Reserve Estimation, Elsevier Science, New York, 364 pp.

Deutsch, C.V. & Journel, A.G. 1998. Geostatistical Software Library and User's Guide. 2nd ed. New York: Oxford University Press.

Di Martino, R., Capasso, G., M. Camarda, M., De Gregorio, S., & Prano, V. 2020. Deep $CO_2$ release revealed by stable isotope and diffuse degassing surveys at Vulcano (Aeolian Islands) in 2015–2018. Journal of Volcanology and Geothermal Research 401. https://doi.org/10.1016/j.jvolgeores.2020.106972

Di Martino, R., Gurrieri, S., Camarda, M., Capasso, G., & Prano, V. 2022. Hazardous Changes in Soil $CO_2$ Emissions at Vulcano, Italy, in 2021. Journal of Geophysical Research: Soil Earth. https://doi.org/10.1029/2022JB024516

Edmonds, M., Grattan, J., & Michnowicz, S. 2015. Volcanic gases: silent killers. In Observing the Volcano World (pp. 65-83). Springer, Cham. https://doi.org/10.1007/11157_2015_14

Ego, F., Sébrier, M., Lavenu, A., Yepes, H., & Egues, A. 1996. Quaternary state of stress in the Northern Andes and the restraining bend model for the Ecuadorian Andes. Tectonophysics, 259. https://doi.org/10.1016/0040-1951(95)00075-5

Egüez, A. & Albán, A. 2017. Mapa geológico de la República del Ecuador. Geological Map of the Republic of Ecuador), Instituto de Investigación Geológico y Energético, Quito, Ecuador.

Eguez, A., Alvarado, A., Yepes, H., Machette, M. N., Costa, C., Dart, R. L., & Bradley, L. A. 2003. Database and map of Quaternary faults and folds of Ecuador and its offshore regions. US Geological Survey Open-File Report, 3, 289.

Etiope, G., Beneduce, P., Calcara, M., Favali, P., Frugoni, F., Schiattarella, M., & Smriglio, G. 1999. Structural pattern and $CO_2$–$CH_4$ degassing of Ustica Island, Southern Tyrrhenian basin. Journal of Volcanology and Geothermal Research, 88(4), 291-304.

Farrar, C.D., Sorey, M.L., Evans, W.C., Howle, J.F., Kerr, B.D., Kennedy, B.M., King, C.-Y., & Southon, J.R. 1995. Forest-killing diffuse $CO_2$ emission at Mammoth Mountain as a sign of magmatic unrest. Nature 376, 675-678 https://doi.org/10.1038/376675a0

Favara, R., Giammanco, S., Inguaggiato, S., & Pecoraino, G. 2001. Preliminary estimate of $CO_2$ output from Pantelleria Island volcano (Sicily, Italy): evidence of active mantle degassing. Applied Geochemistry, 16, 883-894.

Fischer, T.P., Arellano, S., Carn, S., Aiuppa, A., Galle, B., Allard, P., Lopez, T., Shinohara, H., Kelly, P., Werner, C., Cardellini, C., & Chiodini, G. 2019. The emissions of $CO_2$ and other volatiles from the world's subaerial volcanoes. Scientific Reports 9. https://doi.org/10.1038/s41598-019-54682-1

Frondini, F., Chiodini, G., Caliro, S., Cardellini, C., Granieri, D., & Ventura, G. 2004. Diffuse $CO_2$ degassing at Vesuvio, Italy. Bulletin of volcanology, 66, 642-651

Giammanco, S., Melián, G., Neri, M., Hernández, P., Sortino, F., Barrancos, J., López, M., Pecoraino, G., & Perez, N. 2016. Active tectonic features and structural dynamics of the summit area of Mt. Etna (Italy) revealed by soil $CO_2$ and soil temperature surveying. Journal of Volcanology and Geothermal Research 311: 79 – 98. http://dx.doi.org/10.1016/j.jvolgeores.2016.01.004

Gurrieri, S., Di Martino, R., Camarda, M., & Francofonte, V. 2023. Monitoring $CO_2$ Hazards of Volcanic Origin: A Case Study at the Island of Vulcano (Italy) during 2021–2022. Geosciences 13. https://doi.org/10.3390/geosciences13090266

Gutscher, M.A., Malavieille, J., Lallemand, S., & Collot, J.Y. 1999. Tectonic segmentation of the North Andean margin: impact of the Carnegie Ridge collision. Earth and Planetary Science Letters 168: 255–270. https://doi.org/10.1016/S0012-821X(99)00060-6

Hall, M. L. & Beate, B. 1991. El volcanismo plio-cuaternario en los Andes del Ecuador. *Estudios Geograficos*, *4*, 5-38.

Hall, M. L., Samaniego, P., Le Pennec, J. L., & Johnson, J. B. 2008. Ecuadorian Andes volcanism: A review of Late Pliocene to present activity, Journal of Volcanology and Geothermal Research, 176. https://doi.org/10.1016/j.jvolgeores.2008.06.012.

Hall, M.L. & Hillebrandt, C., 1988. Mapa de peligros volcánicos potenciales asociados con el volcán Pululahua, Provincia de Pichincha (1:50000). Map of potential volcanic hazards associated with the Pululahua volcano, Pichincha Province.

Hall, M.L., 1977. El volcanismo en el Ecuador. Volcanism in Ecuador. IPGH, Sección Nacional del Ecuador.

Hansell, A. & Oppenheimer, C. 2004. Health hazards from volcanic gases: a systematic literature review. Archives of Environmental Health: An International Journal, 59: 628-639. https://doi.org/10.1080/00039890409602947.

Hernández P.A., Pérez, N.M., Fridriksson, T., Egbert, J., Ilyinskaya, E., Thárhallsson, A., Ívarsson, G., Gíslason, G., Gunnarsson, I., Jónsson, B., Padrón, E., Melián, G., Mori, T., & Notsu, K. 2012. Diffuse volcanic degassing and thermal energy release from Hengill volcanic system, Iceland. Bulletin of Volcanology 74:2435-2448. https://doi.org/10.1007/s00445-012-0673-2.

Hernández Perez, P., Notsu, K., Tsurumi, M., Mori, T., Ohno, M., Shimoike, Y., Salazar, J., & Pérez, N. 2003. Carbon dioxide emissions from soils at Hakkoda, north Japan. Journal of Geophysical Research: Solid Earth, 108. https://doi.org/10.1029/2002JB001847.

Hernández, P. A., Salazar, J. M., Shimoike, Y., Mori, T., Notsu, K., & Pérez, N. 2001a. Diffuse emission of $CO_2$ from Miyakejima volcano, Japan. Chemical Geology, 177(1-2), 175-185.

Hernández, P.A., Notsu, K., Okada, H., Mori, T., Sato, M., Barahona, F., & Pérez, N.M. 2006. Diffuse emission of $CO_2$ from Showa-Shinzan, Hokkaido, Japan: A sign of volcanic dome degassing. Pure and Applied Geophysics 163(4):869-881, doi: 10.1007/s00024-006-0038-x

Hernández, P.A., Notsu, K., Salazar, J.M., Mori, T., Natale, G., Okada, H., Virgili, G., Shimoike, Y., Sato, M., & Pérez, N.M. 2001b. Carbon dioxide degassing by advective flow from Usu volcano, Japan. Science 292:83-86.

Hidalgo, S., Bernard, B., Mothes, P., Ramos, C., Aguilar, J., Andrade, D., Samaniego, P., Samaniego, P., Yepes, H., Hall, M., Alvarado, A., Segovia, M., Ruiz, M., Ramón, P., Vaca, M., & IG-EPN staff. 2024. Hazard assessment and monitoring of Ecuadorian volcanoes: challenges and progresses during four decades since IG-EPN foundation. Bulletin of Volcanology 86, 4. https://doi.org/10.1007/s00445-023-01685-6.

IG-EPN. 2016. Medición de parámetros fisicoquímicos en aguas termales y fuentes de gas del Complejo Volcánico Pululahua. Technical report.

Hoefs, J. 2004. Stable Isotope Geochemistry. 6th Edition. Springer-Verlag, 274 pp.

Ingebritsen, S. E., & Ziagos, J. S. 1995. Permeability of the continental crust: Dynamic variations inferred from seismicity and metamorphism. Journal of Geophysical Research: Solid Earth 100 (B7): 12831-12848.

Inguaggiato, S., Mazot, A., Diliberto, I.S., Inguaggiato, C., Madonia, P., Rouwet, D., & Vita, F. 2012. Total $CO_2$ output from Vulcano island (Aeolian Islands, Italy). Geochemistry, Geophysics, Geosystems 13. https://doi.org/10.1029/2011GC003920.

Inguaggiato, S., Hidalgo, S., Beate, B., Bourquin, J. 2021. Geochemical and isotopic characterization of volcanic and geothermal fluids discharged from the Ecuadorian volcanic arc. Geofluids. https://doi.org/10.1111/j.1468-8123.2010.00315.x.

IVHHN, 2016. Carbon Dioxide (CO2). The International Volcanic Health Hazard Network Website. Copyright © 2016. Consultado el 06/06/16. Available at: http://www.ivhhn.org/index.php?option=com_content&view=article&id=84.

Kis, B.M., Ionescu, A., Cardellini, C., Harangi, Sz., Baciu, C., Caracausi, A., & Viveiros F. 2017. Quantification of carbon dioxide emissions of Ciomadul, the youngest volcano of the Carpathian-Pannonian Region (Eastern-Central Europe, Romania). Journal of Volcanology and Geothermal Research Volume 341: 119-130 https://doi.org/10.1016/j.jvolgeores.2017.05.025.

Lages, J., Rizzo, A.L., Aiuppa A., Robidoux, P., Aguilar, R., Apaza, F., Masias P. 2021. Crustal controls on light noble gas isotope variability along the Andean Volcanic Arc. Geochemical Perspectives Letters 19, 45–49. doi: 10.7185/geochemlet.2134.

Lamberti, M.C., Agusto, M., Llano, J., Nogués, V., Vélez, M.L., Albite, J.M., Yiries, J., Chiodini, G., Cardellini, C., Tassi, F., García, S., Nuñez, N., Sánchez, H., & Gómez, M. 2021. Soil $CO_2$ flux baseline in Planchón – Peteroa Volcanic Complex, Southern Andes, Argentina. Journal of South American Earth Sciences. ALVO Conference Special Issue. https://doi.org/10.1016/j.jsames.2020.102930.

Lamberti, M.C., Forte, P., Llano, J., & Agusto, M. 2021. Living with volcanic gases: the complex challenge facing the town of Copahue, province of Neuquén (Conviviendo con gases volcánicos: el complejo desafío que afronta la localidad de Copahue, provincia de Neuquén). II Conference on Fundamentals and Applications of Interdiscipline, virtual congress, Argentina.

Lamberti, M.C., Vigide, N., Venturi, S., Agusto, M., Yaguspky, D., Winocur, D., Barcelona, H., Vélez, M.V., Cardellini, C., & Tassi, F. 2019. Structural architecture releasing deep-sourced carbon dioxide diffuse degassing at the Caviahue – Copahue Volcanic Complex. Journal of Volcanology and Geothermal Research, 374: 131 – 141. https://doi.org/10.1016/j.jvolgeores.2019.02.004.

Le Guern, F., Tazieff, H., & Pierret, R. F. 1982. An example of health hazard: people killed by gas during a phreatic eruption: Dieng Plateau (Java, Indonesia), February 20th 1979. Bulletin Volcanologique, 45: 153 – 156. https://doi.org/10.1007/BF02600430.

Lewicki, J., Bergfeld, D., Cardellini, C., Chiodini, G., Granieri, D., Varley, N., Werner, C. 2005. Comparative soil $CO_2$ flux measurements and geostatistical estimation methods on Masaya volcano, Nicaragua. Bulletin of Volcanology, 68(1). https://doi.org/10.1007/s00445-005-0423-9.

Li Vigni, L., Cardellini, C., Temovski, M., Ionescu, A., Molnár, K., Palcsu, L., Gagliano, A. L., Cappuzzo, S., & D'Alessandro W. 2022. Duvalo "volcano" (North Macedonia): A purely tectonicrelated $CO_2$ degassing system. Geochemistry, Geophysics, Geosystems, 23, e2021GC010198. https://doi.org/10.1029/2021GC010198.

Lopez, L., Aguilera, F., Tassi, F., de Moor, M., Bobrowski, N., Aiuppa, A., Tamburello, G., Rizzo, A., Liuzzo, M., Viveiros, F., Cardellini, C., Silva, C., Fischer, T., Jean-Baptiste, P., Kazayaha, R., Hidalgo, S., Malowany, K., Lucic, G., Bagnato, Bergsson, B., Reath, K., Liotta, M., Carn, S., & Chiodini, G. 2018. New insights into the magmatic-hydrothermal system and volatile budget of Lastarria volcano, Chile: Integrated results from the 2014 IAVCEI CCVG 12th Volcanic Gas Workshop. Geosphere 14 (3). https://doi.org/10.1130/GES01495.1

Ministerio del Ambiente, Agua y Transición Ecológica (MAATE). 2015. Reserva Geo-Botánica Pululahua, Biodiversidad. Quito-Ecuador. www.areasprotegidas.gob.ec

Marrero, R., López, D. L., Hernández, P. A., & Pérez, N. M. 2008. Carbon dioxide discharged through the las Cañadas aquifer, Tenerife, Canary Islands. Pure and Applied Geophysics, 165, 147-172.

Mazot, A., Smid, E., Schwendenmann, L., Delgado-Granados, H., & Lindsay, J. 2013. Soil $CO_2$ flux baseline in an urban monogenetic volcanic field: the Auckland Volcanic Field, New Zealand. Bulletin of Volcanology 75: 757. https://doi.org/10.1007/s00445-013-0757-7.

McKnight, J. Y., Harden, C. P., & Schaeffer, S. M. 2016. Soil $CO_2$ flux trends with differences in soil moisture among four types of land use in an Ecuadorian páramo landscape. Physical Geography, 38(1), 51–61. https://doi.org/10.1080/02723646.2016.1256101.

Melián, G., Somoza, L., Padrón, E., Pérez, N., Hernandez, P., Sumino, H., Forjaz, V., & Franca, Z. 2016. Surface $CO_2$ emission and rising bubble plumes from degassing of crater lakes in São Miguel Island, Azores. Geological Society London Special Publications 437(1). https://doi.org/10.1144/SP437.14.

Melián, G., Toulkeridis, T, Pérez, N., Hernandez, P., Somoza, L, Padrón, E., Amonte C., Alonso, M., Asensio-Ramos, M., & Cordero, M. 2021. Geochemistry of Water and Gas Emissions From Cuicocha and Quilotoa Volcanic Lakes. Frontiers in Earth Science. 9:741528. https://doi:10.3389/feart.2021.741528.

Melián, G., Tassi, F., Pérez, N., Hernández, P., Sortino, F., Vaselli, O., Padrón, E., Nolasco, D., Barrancos, J., Padilla, G., Rodríguez, F., Dionis, S., Calvo, D., Notsu, K., & Sumino, H. 2012. A magmatic source for fumaroles and diffuse degassing from the summit crater of Teide Volcano (Tenerife, Canary Islands): a geochemical evidence for the 2004–2005 seismic–volcanic crisis. Bulletin of Volcanology, 74(6): 1465–1483. https://doi.org/10.1007/s00445-012-0613-1.

Mook, W.G. 2002. Environmental Isotopes in the Hydrological Cycle. Principles and Applications International Atomic Energy Agency and United Nations Educational, Scientific and Cultural Organization, 185 pp. Amsterdam.

NIOSH, 1981. Occupational Health Guidelines for Chemical Hazardous, National Institute of Occupational Safety and Health. Cincinnati, OH, U.S.A.

Oliveira, S., Viveiros, F., Silva, C., & Pacheco, J.E. 2018. Automatic filtering of soil $CO_2$ flux data; different statistical approaches applied to long time series. Frontiers in Earth Science, 6: 208. https://doi.org/10.3389/feart.2018.00208.

Ono, A., Sano, Y., Wakita, H., & Giggenbach, W.F. 1993. Carbon isotopes of methane and carbon dioxide in hydrothermal gases of Japan. Geochemical Journal 27: 287-295.

Padilla, G., Alonso, M., Morales, C., Ibarra, M., Espinoza, E., Hernández, P., Barrancos, J., Rodríguez, F., Melián, G., Calvo, D., Padrón, E., Martínez, W., Saballos, A., & Pérez, N. 2018. Monitoring diffuse $CO_2$ degassing at Masaya caldera, Nicaragua. Geophysical Research Abstracts Vol. 20, EGU2018-17507-2, EGU General Assembly 2018.

Padrón, E., Hernández, P. A., Pérez, N. M., Toulkeridis, T., Melián, G., Barrancos, J., Virgilli, G., Sumino, H., & Notsu, K. 2012. Fumarole/plume and diffuse $CO_2$ emission from Sierra Negra caldera, Galapagos archipelago. Bulletin of volcanology, 74, 1509-1519.

Padrón, E., Hernández, P.A., Toulkeridis, T., Pérez, N.M., Marrero, R., Melián, G., Virgili, G., & Notsu, K. 2008. Diffuse $CO_2$ emission rate from Pululahua and the lake-filled Cuicocha calderas, Ecuador. Journal of Volcanology and Geothermal Research 176, 163–169. https://doi.org/10.1016/j.jvolgeores.2007.11.023.

Pallini, R. 1996. Studio stratigrafico e granulometrico di un deposito di ricaduta da colonna pliniana in assenza di vento (vulcano Pululagua, Ecuador). The stratigraphic and granulometric study of a deposit fallen from plinian coloumn in the absence of wind Università di Pisa, Pisa.

Papale, P. & Rosi, M., 1993. A case of no-wind plinian fallout at Pululahua caldera (Ecuador): implications for models of clast dispersal. Bull. Volcanol. 55, 523–535. https://doi.org/10.1007/BF00304594.

Ramon, P., Vallejo Vargas, S., Mothes, P. A., Andrade, S. D., Vasconez, F. J., Yepes, H., Hidalgo, S., & Santamaría, S. 2021. Instituto Geofísico – Escuela Politécnica Nacional, The Ecuadorian Seismology and Volcanology Service, 4, 93–112.

Rice, J. A. 2007. Mathematical statistics and data analysis, 3rd Edition. Cengage Learning. 603 pp.

Salazar, J. M., Hernández, P. A., Pérez, N. M., Melián, G., Álvarez, J., Segura, F., & Notsu, K. 2001. Diffuse emission of carbon dioxide from Cerro Negro volcano, Nicaragua, Central America. Geophysical Research Letters, 28(22), 4275-4278.

Salazar, J. M., Hernández, P. A., Pérez, N. M., Olmos, R., Barahona, F., Cartagena, R., Soriano, T., López, D., Sumino, H., Notsu, K. 2004. Spatial and temporal variations of diffuse $CO_2$ degassing at the Santa Ana–Izalco–Coatepeque volcanic complex, El Salvador, Central America. Natural Hazards in El Salvador. https://doi.org/10.1130/0-8137-2375-2.135.

Sánchez, M.E., Chimner, R.A., Hribljan, J.A., Lilleskov, E.A., & Suárez, E. 2017. Carbon dioxide and methane fluxes in grazed and undisturbed mountain peatlands in the Ecuadorian Andes. Mires and Peat. 19: art. 20. 18 p. https://doi.org/10.19189/MaP.2017.OMB.277.

Santamaría, S., Telenchana, E., Bernard, B., Hidalgo, S., Beate, B., Córdova, M., & Narvaez, D. 2017. Registro de erupciones ocurridas en los Andes del Norte durante el Holoceno: Nuevos resultados obtenidos en la turbera de Potrerillos, Complejo Volcánico Chiles-Cerro Negro. Record of eruptions that occurred in the Northern Andes during the Holocene: New results obtained in the Potrerillos peat bog, Chiles-Cerro Negro Volcanic Complex. Revista Politécnica.

Schlesinger, R.B. & Cassee, F. 2003. Atmospheric secondary inorganic particulate matter: the toxicological perspective as a basis for health effects risk assessment. Inhalation Toxicology 15(3):197-235. https://doi.org/10.1080/08958370304503.

Shimoike, Y., Kazahaya, K., & Shinohara, H. 2002. Soil gas emission of volcanic $CO_2$ at Satsuma-Iwojima volcano, Japan. Earth, planets and space, 54(3), 239-247.

Sierra, D. 2022. Estudios geoquímicos de fluidos de los sistemas volcánicos e hidrotermales activos del Norte de los Andes Ecuatorianos. PhD Thesis, 30p., University of Buenos Aires, Argentina.

Sierra, D., Hidalgo, S., Almeida, M., Vigide, N., Lamberti, M.C., Proaño, A., & Narvaez, D. 2020. Temporal and spatial variations on $CO_2$ diffuse volcanic degassing on Cuicocha Caldera Lake - Ecuador. Journal of Volcanology and Geothermal Research. https://doi.org/10.1016/j.jvolgeores.2020.107145.

Sinclair A.J. 1974. Selection of threshold values in geochemical data using probability graphs. Journal of Geochemical Exploration 3: 129– 149.

Smets, B., Tedesco, D., Kervyn, F., Kies, A., Vaselli, O., & Yalire, M. 2010. Dry gas vents (“mazuku”) in Goma region (North-Kivu, Democratic Republic of Congo): Formation and risk assessment. Journal of African Earth Sciences, 58(5), 787-798. https://doi.org/10.1016/j.jafrearsci.2010.04.008.

Sorey, M. L., Evans, W. C., Kennedy, B. M., Farrar, C. D., Hainsworth, L. J., & Hausback, B. 1998. Carbon dioxide and helium emissions from a reservoir of magmatic gas beneath Mammoth Mountain, California. Journal of Geophysical Research: Solid Earth, 103, 15303-15323.

Toutain, J.P., Sortino, F., Baubron, J.C., Richon, P., Surono, Sumarti, S., & Nonell, A. 2009. Structure and $CO_2$ budget of Merapi volcano during inter-eruptive periods. Bull Volcanol 71(7):815-826. https://doi.org/10.1007/s00445-009-0266-x.

USGS, 2016. Volcanic gases can be harmful to health, vegetation and infrastructure. United States Geologic Service Website. Page modified: 2016-02-12 09:40. Reviewed: 07/06/2016. Available in: https://volcanoes.usGs.gov/vhp/gas.html.

Vásconez Müller, A., Cashman, K.V., Mitchell, S.J., & Vasconez, F. 2022. The 2.6–2.3 ka explosive eruptive period of the Pululahua dome complex, Ecuador: insights from pyroclast analysis. Bulletin of Volcanology 84, 81. https://doi.org/10.1007/s00445-022-01590-4.

Vasconez, F. 2019. Exposure-based risk analysis in case of a Plinian eruption (VEI 4) of Pululahua Volcanic Complex, Ecuador. Thesis for the Specialisation Certificate in the Assessment and Management of Geological and Climate Related Risk, Geneva University, Geneva. 38 pp.

Vasconez, F., Bonadonna, C., Frischknecht, C., & Andrade, D. 2019. Exposure-based risk analysis in case of a Plinian eruption (VEI 4) of Pululahua Volcanic Complex, Ecuador. IUGG 2019, V04p-164.

Venturi, S., Tassi, F., Cabassi, J., Vaselli, O., Minardi, I., Neri, S., Caponi, C., Capasso, G., Di Martino, R., Ricci, A., Capecchiacci, F., Lelli, M., Sciarra, A., Cinti, D., & Virgili, G. 2019. A multi-instrumental geochemical approach to assess the environmental impact of $CO_2$-rich gas emissions in a densely populated area: The case of Cava dei Selci (Latium, Italy). Applied Geochemistry 101:109-126. https://doi.org/10.1016/j.apgeochem.2019.01.003.

Viveiros, F., Cardellini, C., Ferreira, T., Caliro, S., Chiodini, G., & Silva, C. 2010. Soil $CO_2$ emissions at Furnas volcano, São Miguel Island, Azores archipelago: Volcano monitoring perspectives, geomorphologic studies, and land use planning application. Journal of Geophysical Research 115, B12208. https://doi.org/10.1029/2010JB007555.

Viveiros, F., Chiodini, G., Cardellini, C., Caliro, S., Zanon, V., Silva, C., Rizzo, A., Hipólito, A., & Moreno, L. 2020. Deep $CO_2$ emitted at Furnas do Enxofre geothermal area (Terceira Island, Azores archipelago). An approach for determining $CO_2$ sources and total emissions using carbon isotopic data, Journal of Volcanology and Geothermal Research 401. https://doi.org/10.1016/j.jvolgeores.2020.106968.

Viveiros, F., Ferreira, T., Silva, C., & Gaspar, J.L. 2009. Meteorological factors controlling soil gases and indoor $CO_2$ concentration: A permanent risk in degassing areas. Science of the Total Environment, 407, 1362-1372. https://doi.org/10.1016/j.scitotenv.2008.10.009.

Viveiros, F., Ferreira, T., Vieira, J. C., Silva, C., & Gaspar, J. L. 2008. Environmental influences on soil $CO_2$ degassing at Furnas and Fogo volcanoes (São Miguel Island, Azores archipelago). Journal of Volcanology and Geothermal Research, 177(4), 883-893. https://doi.org/10.1016/j.jvolgeores.2008.07.005.

Viveiros, F., Gaspar, J., Ferreira, T., & Silva, C. 2016. Hazardous indoor $CO_2$ concentrations in volcanic environments. Environmental Pollution, Volume 214. https://doi.org/10.1016/j.envpol.2016.04.086.

Volentik, A.C.M., Bonadonna, C., Connor, C.B., Connor, L.J., & Rosi, M. 2010. Modeling tephra dispersal in absence of wind: Insights from the climactic phase of the 2450 BP Plinian eruption of

Pululagua volcano (Ecuador). Journal of Volcanology and Geothermal Research 193, 117–136. https://doi.org/10.1016/j.jvolgeores.2010.03.011.

Werner, C. & Brantley, S. 2003. $CO_2$ emissions from the Yellowstone volcanic system. Geochemistry, Geophysics, Geosystems, 4(7).

Werner, C. & Cardellini, C. 2006. Comparison of carbon dioxide emissions with fluid upflow, chemistry, and geologic structures at the Rotorua geothermal system, New Zealand. Geothermics, 35(3). https://doi.org/10.1016/j.geothermics.2006.02.006.

Werner, C., Fischer, T., Aiuppa, A., Edmonds, M., Cardellini, C., Carn, S., Chidini, G., Cottrell, Burton, M., & Allard, P. 2019. Carbon Dioxide Emissions from Subaerial Volcanic Regions: Two Decades in Review. In B. Orcutt, I. Daniel, & R. Dasgupta (Eds.), Deep Carbon: Past to Present (pp. 188-236). Cambridge: Cambridge University Press. https://doi.org/10.1017/9781108677950.

Williams-Jones, G. & Rymer, H. 2015. Hazards of volcanic gases. In The Encyclopedia of Volcanoes (Second Edition) 985-992. https://doi.org/10.1016/B978-0-12-385938-9.00057-2.

**STATEMENT**

The authors have no competing interests to declare.

**Declaration of interests**

☐The authors declare that they have no known competing financial interests or personal relationships that could have appeared to influence the work reported in this paper.

☒The authors declare the following financial interests/personal relationships which may be considered as potential competing interests:

| |
|---|
| Daniel Sierra, Francisco Vasconez, and Silvana Hidalgo reports financial support was provided by SENESCYT and BID. Carlo Cardellini reports financial support was provided by Deep Carbon Observatory. Carlo Cardellini reports was provided by Italian Ministry of Ministry of University and Research. Fatima Viveiros and Catarina Silva reports financial support was provided by Portuguese FCT funding agency. If there are other authors, they declare that they have no known competing financial interests or personal relationships that could have appeared to influence the work reported in this paper. |

**Highlights**

- Pululahua emits volcanic $CO_2$ diffuse degassing from its crater
- Diffuse degassing structures form a circular shape around the youngest domes
- Carbon isotopic composition of $CO_2$ indicates both biological and volcanic sources
- Volcanic output is 59 - 97 t $d^{-1}$, based on criteria for subtracting biological $CO_2$
- Probability map of fluxes above the biogenic threshold approximates a hazard map